ISTITUTO NAZIONALE DI GEOFISICA E VULCANOLOGIA

ACCEPTED ON ANNALS OF GEOPHYSICS, 61, 2018; Doi: 10.4401/ag-7859

Advances in the rheology of natural multiphase silicate melts: Import for magma transport and lava flow emplacement

Daniele Giordano[1, 2, 3]

1) Università degli Studi di Torino, Dipartimento di Scienze della Terra, Via Valperga Caluso 35, 10125 Torino, Italy
2) Istituto Nazionale di Geofisica e Vulcanologia-Sezione di Pisa, Via della Faggiola, 32,
56126 Pisa, Italy.
3) Institute of Geoscience and Earth Resources (IGG-CNR), Italian National Research
Council (CNR), Pisa, Italy;

Advances in the rheology of natural multiphase silicate melts: Importance for magma transport and lava flow emplacement

D. Giordano[1, 2, 3]

1) Università degli Studi di Torino, Dipartimento di Scienze della Terra, Via Valperga Caluso 35, 10125 Torino, Italy

2) Istituto Nazionale di Geofisica e Vulcanologia-Sezione di Pisa, Via della Faggiola, 32, 56126 Pisa, Italy.

3) Institute of Geoscience and Earth Resources (IGG-CNR), Italian National Research Council (CNR), Pisa, Italy;

Submitted to: Annals of Geophysics

Special volume: "MeMoVolc"

Corresponding author: Daniele Giordano: daniele.giordano@unito.it

Keywords: Multicomponent and Multiphase silicate melts, Rheology,

Abstract

A review of recent advances in the field of rheology of multicomponent silicate melts and multiphase silicate melt suspensions is presented here. The advances include the development of new experimental devices and field and remote sensing methods for measuring the rheological properties of natural melts and magmas. These promising approaches combine laboratory experiments, theoretical models, numerical simulations and remote sensing data derived from ground, airborne and satellite-based tools. Each of these sub-disciplines has evolved rapidly in recent years and the growing range of complementary data appears now to provide an opportunity for the development of multi-disciplinary research. Ultimately, these multidisciplinary initiatives seek to provide near-real-time forecasting of hazardous volcanic processes such as lava flow field evolution. The results and approaches described here focus on multiphase (i.e. melts, bubbles, crystals) rheology of natural systems and are pertinent to the effusive emplacement of lavas, dykes and sills, as well as, to the eruption dynamics attending explosive eruptions.

Keywords: Multicomponent and Multiphase silicate melts, Rheology,

1. Introduction

The transport of magmas and volcanic materials is characterized by very dynamic, interdependent and complex, physical and chemical processes that all are affected by and affect the materials physical properties. Understanding the dynamic processes operating during magma ascent and eruption and the timescales and mechanisms of emplacement, welding and remobilization of fragmental or massive volcanic deposits, constitutes one of the main challenges in the Earth sciences (Dingwell, 1996; Papale, 1999; Sparks, 2004; Russell and Quane, 2005; Giordano et al., 2005). Accurate description of these processes requires the characterization of a wide range of transport and thermodynamic properties for the melt or magma (e.g. viscosity, density, enthalpy, entropy, heat capacity, thermal conductivity, solubility of volatile phases). These properties play crucial roles at micro- to macroscopic scale and many are correlated, in a non-linear manner (e.g. Richet et al., 1984; Giordano et al., 2008a; Russell and Giordano, 2017).

Lava flow dynamics are strongly governed by subsurface buoyancy forces, resulting from the density contrast with the host rock, which push the magma toward the surface (e.g. Wilson & Head, 2016a; Wieczorek et al. 2001), and by the evolving internal and external frictional forces (e.g. with dyke, conduit wall and topography) that oppose to the movement of magmas and lavas (e.g. Nemeth, 2010; Cañón-Tapia, 2016, Dragoni, 1993; Dragoni et al. 2005; Giordano et al., 2007; Cashman et al., 2013; Kolzenburg et al., 2016a,b; 2018a,b; Hulme, 1974; Hiesinger et al., 2007, Chevrel et al., 2013, 2015, Castruccio et al. 2014).

The rheological properties of magmas undergo tremendous changes from transport in the subsurface to eruption or emplacement at the surface and to final deposition and cooling. These changes are caused dominantly by the evolving of thermo-chemical and deformational conditions, imposing phase transitions and therewith heterogeneous textural and morphological variations of the magmatic and volcanic suspensions which evolve in space and time. The complex rheological evolution of lava flows can tentatively be constrained by carrying out laboratory measurements

under controlled conditions, simulating natural systems, and by monitoring flow emplacement at the field-scale and via satellite-based platforms. In parallel with this, the sophistication of physical models of lava flows and domes have improved significantly and are capable of providing fast simulations (see, amongst the others, Costa and Macedonio, 2003, 2005; Del Negro et al, 2008, 2013, 2016; Melnik and Sparks, 1999, 2005; Melnik et al., 2009; Kilburn 2015 for reviews on this topic). These models are increasingly informed by, or validated by, satellite-derived parameters such as lava flow discharge rate or periodic updates on flow advance/geometry. Together these capabilities represent an emergent strategy that may provide timely reliable projections of lava flow field evolution and derive information for hazard assessment and mitigation measures. Yet, to date they do not always provide coherent results reproduced in nature.

This highlights the necessity to estimate the rheological properties of magmas and volcanic materials at conditions pertinent to nature and to investigate the effect of each variable over the range of relevant environmental conditions (e.g. pressure, temperature, volatile contents) during varying thermodynamic (equilibrium and non-equilibrium) conditions, and deformation regimes.

Our understanding of the single- and multi-phase (liquid+crystals+bubbles) rheology of magmas and volcanic products has greatly improved in the last two decades. This can largely be attributed to the growing availability of empirical data from the following sources (each of which will be reviewed in detail below):

1) laboratory experimentation on natural and simplified silicate melts. These data support the creation of robust models for predicting the Newtonian viscosity of pure liquid natural melts as a function of temperature (T), pressure (P) composition (X), volatile content (X_v) and structural features (see Chapter 2).

2) the rheological experimentation and modelling of non-reactive multiphase suspensions (liquid+bubbles; liquid+crystal and liquids+bubbles+crystals) constituted by analogue materials or simplified or natural silicate melts mixtures (Chapter 4);

3) dynamic cooling rheological measurements on natural multiphase suspensions at non-isothermal and non-equilibrium conditions to explore the interdependent effects of composition, cooling-rate, shear-rate and oxygen fugacity acting during magma and lava transport in nature (Chapter 5);

4) rheological measurements of actively flowing lava. These represent snapshots of actual lava flow rheology at specific conditions and provide data that helps to constrain the conditions required to be reproduced in systematic laboratory studies (Chapter 6).

5) studies on the 3D and 4D evolution of lava flows at increasing spatial and temporal resolution and contemporary estimates of effusion rate and flow development from satellite data. These provide data for cross correlation and benchmarking of laboratory measurements (Appendix A1) and to re-visit long standing methods for deriving rheological parameters from morphologic data (Chapter 6).

These studies document that the effective viscosity of natural silicate melts and magmas can span more than 15 orders of magnitude (10^{-1} – 10^{14} Pa s), primarily in response to variations in melt composition (X), dissolved volatile content (Xv), temperature (T), pressure (P), as well as the proportions, size, and shape distributions of suspended solid and/or exsolved fluid phases (i.e. crystals and bubbles). The deformation rate, which in nature would depend on the discharge rate will determine whether flow behavior will be Newtonian (i.e. one for which there is a linear relationship between stress and strain rate; or spatial variation of velocity) or non-Newtonian (e.g. Caricchi et al., 2007, 2008; Costa et al., 2007a, 2009; Vona et al. 2011, Hess et al., 2009). Deformation rate also exerts an influence on the crystallization kinetics (Vona et al., 2013, Kouchi,

106 1986, Kolzenburg 2018). It may further determine whether the melt will deform viscously or
107 elastically and, therewith, whether or not it will eventually fracture giving origin to effusive rather
108 than explosive eruptive styles (Dingwell, 1996). Combined the above experimental data and
109 computational models form a basis from which to understand the flow behavior of natural magmatic
110 and volcanic suspensions.

111 In the following I present a review of the research advances in the rheological
112 characterization of pure silicate melts and multiphase silicate mixtures (i.e. lavas and magmas)
113 achieved in the past decades. I follow the structure of points 1-5 outlined above to group the
114 individual fields. In the Appendices (A1-A3) I summarize the most commonly employed
115 experimental devices and technological advances to measure the single and multiphase silicate
116 melts also reporting the most common equations used to describe the viscosity variation as a
117 function of P, T, X (Appendix A1) as well as suspended solids phase and/or porosity (Appendices
118 A2 and A3). I conclude with a discussion of how new laboratory developments and of the growth in
119 complementary datasets (e.g. remote-sensing; drone technology; high-speed calculation facility) is
120 providing greater understanding of magma and lava transport on Earth.

121

122 **2. Pure liquid melt Newtonian viscosity experiments and models**

123 ***2.1. T – dependent models for predicting melt viscosity***

124 The first step toward characterizing multiphase rheology of natural silicate melts mixture is
125 the knowledge of multicomponent viscosity of pure liquids as a function of their composition
126 (including dissolved volatile species such as H_2O, C and S –species, F, Cl) temperature (T) and
127 pressure (P). Early models for predicting the viscosity of silicate melts were developed using data
128 that spanned relatively small ranges of temperature (T) and viscosity (η). These experimental data,
129 restricted to superliquidus temperatures and a narrow compositional range, showed a nearly linear
130 trend of viscosity in reciprocal temperature space. Thus, early models adopted an Arrhenian

formulation of the temperature-viscosity relationship (Shaw, 1972; Bottinga and Weill, 1972). Expansion of the melt viscometry database over a wider range of compositions and temperatures exposed the limitations of Arrhenian models. With the emergence of viscometry data closer to the glass transition temperature (T_g) (i.e. the temperature of transition between a liquid-like and a solid-like behavior) (e.g. Angell, 1991, Giordano et al., 2005), the Arrhenian models proved unsuitable to describe the temperature dependence of silicate melt viscosity. These measurements were enabled by experimental devices that allow very small displacements to be monitored (e.g. Linear Voltage Displacement Transducers) and, the production of quenched glasses, freezing in the crystal free melt structure. In these experiments, supercooled glasses are reheated above T_g, where the "relaxed melt" viscosity (e.g. Angell, 1991; Scherer, 1984) could then be measured. These experiments are performed at timescales shorter than phase transitions timescale, therewith allowing anhydrous and hydrous pure liquid viscosity measurements (Angell, 1991; Scherer, 1984; Giordano et al., 2008b).

Based on the large number of experimental studies (e.g. Richet et al., 1995; Richet et al., 1996; Hess and Dingwell, 1996; Whittington et al., 2000, 2001; Giordano et al., 2009 amongst the others), models of melt viscosity were developed (e.g. Avramov, 1998; Angell, 1991; Russell et al., 2003; Giordano and Dingwell, 2003a, b; Russell and Giordano, 2005; Giordano and Russell, 2007; Hui and Zhang, 2007; Giordano et al., 2006, 2008a,b; Ardia et al., 2008; Mauro et al., 2009), also accounting for the non-Arrhenian viscosity behaviour (e.g. Vogel, 1921, Fulcher, 1925; Tammann and Hess, 1926; Adam and Gibbs, 1965). These models describe the P-T-X dependence of the viscosity of silicate melts. Some of the most relevant empirical and theoretical formulations describing the T-dependence of silicate melts and the relationships between constitutive parameters are reported in Appendix A2.

The growing database and the new models show that silicate melts display various degrees of non-Arrhenian behavior, from *strong* to *fragile* (Angell, 1991; Russell et al., 2002, 2003), which depend on composition and dissolved volatile content (Fig. 1).

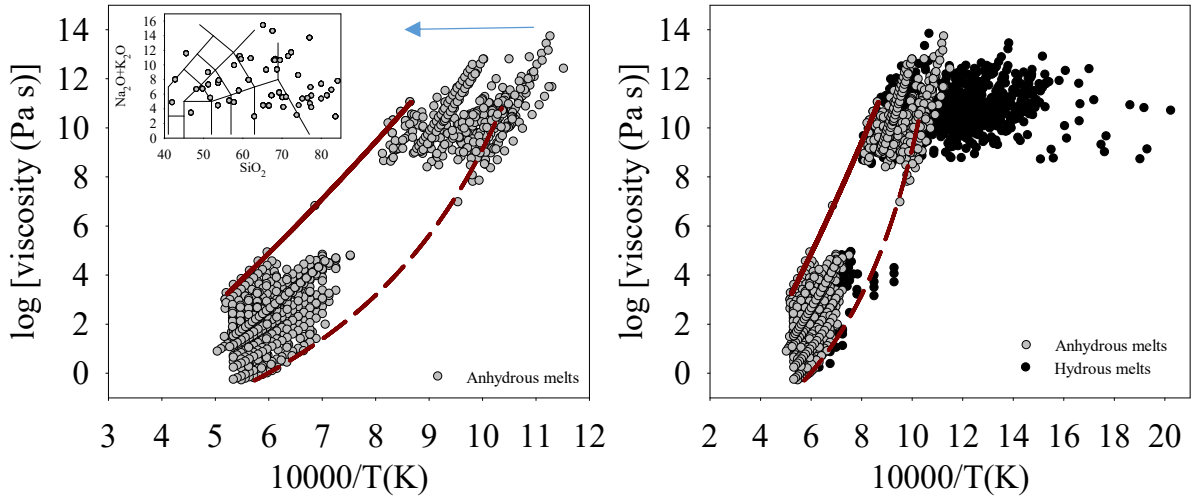

Fig. 1. The figure shows the variation of viscosity as a function of the reverse of temperature for the anhydrous melts (a) and, per comparison, the anhydrous and hydrous melts (b) as reported by Giordano et al. (2008). The curves in a) represent the most Arrhenian (continuous line in a))(strong) and the least Arrhenian (dashed curve in a)) (fragile) melts amongst those reported in panel of Fig 1a. The effect of water is that of significantly reducing viscosity and the fragility (deviation from Arrhenian behavior) of the melts (details in Giordano et al., 2008).

All these models provide viscosity predictions based on composition commonly expressed in terms of oxide abundances or combination of oxides and a range of adjustable parameters. Of the various models only the HZ model (Hui and Zhang, 2007) and the GRD model (Giordano et al., 2008a) accounts for the effects of dissolved volatile species (H_2O, F). The GRD model is based on the well-known VFT (Vogel-Fulcher-Tammann) equation, such that:

$$\log [\eta \text{ (Pa s)}] = A_{VFT}+B_{VFT}/(T-C_{VFT}) \qquad \text{(Eq. 1)}$$

where A_{VFT} is the pre-exponential factor, B_{VFT} is the pseudo-activation energy and C_{VFT} is the VFT-temperature. In contrast the HZ model uses a purely empirical T-dependent viscosity formulation of non straightforward correlation with thermo-physical amounts. The GRD model has gained support due to its simplicity and direct correlation of constitutive parameters (i.e. Appendix A2) to other important physical and structural properties such as the glass transition (T_g), the fragility (m) (i.e. the rate at which viscosity varies with temperature, that is an indication of melts capacity to store energy), calorimetric properties (configurational entropy, Sconf and the configurational heat capacity Cp^{conf}; see Eq A2.4)(e.g. Giordano & Dingwell, 2003a; Giordano et al., 2008b; Chevrel et

al., 2013; Giordano and Russell, 2017; Russell and Giordano, 2017) and structural properties (e.g. Qn-species and Raman Ratio)(i.e. Le Losq and Neuville., 2017; Giordano and Russell, 2018; Giordano et al., 2019). These models show that, to a first approximation, the viscosity of silicate melts can be correlated at constant temperature to empirical, composition-based pseudo-structural parameter (i.e. the SM - structural modifiers - and the NBO/T - i.e. the Non Bridging Oxygen over Tetrahedra - parameters). The NBO/T and SM parameters are commonly assumed as proxies for the degree of polymerization of silicate melts and glasses (e.g Giordano and Dingwell, 2003a, b; Giordano and Russell, 2018; Giordano et al., 2019)(Figs. 2, 3). Compositions with low values of the SM-parameter (or low NBO/T values) are associated to strong (Arrhenian-like) rheological behavior, i.e. a linear behavior in the logη-1/T space, and more polymerized melts. On the other hand high values of SM (or high NBO/Ts) are related to more depolymerized melts which show fragile rheological behavior (i.e. the logη vs 1/T paths are significantly non-linear)(e.g. Angell, 1991; Giordano and Dingwell, 2003)(Figs. 1-2). Russell et al. (2003), in agreement with early theoretical studies (e.g. Angell, 1991 amongst others), showed that the pre-exponential factor of the VFT and AG formulations, i.e. the viscosity at infinite temperature (Appendix A2), is a constant independent of compositions (Russell et al., 2003; Giordano et al., 2008a). The current models are applicable within the compositional space that they are based upon, but some compositional regions (e.g. peralkaline compositions) still remain unmapped and the models struggle to reproduce measured viscosity values (Giordano et al., 2006, 2008a, Di Genova et al., 2017). Those formulations also put in evidence that the role of water (H_2O) dissolved in the melt is counterintuitive being opposite to that of network modifier cations. In fact, although dissolved H_2O strongly decreases the viscosity of silicate melts (Fig 1b), the parameters describing the T-dependence of viscosity (e.g. B_{VFT} and C_{VFT} in Eq. 1) are differently affected by H_2O and by the most common structure modifiers (Fig. 2).

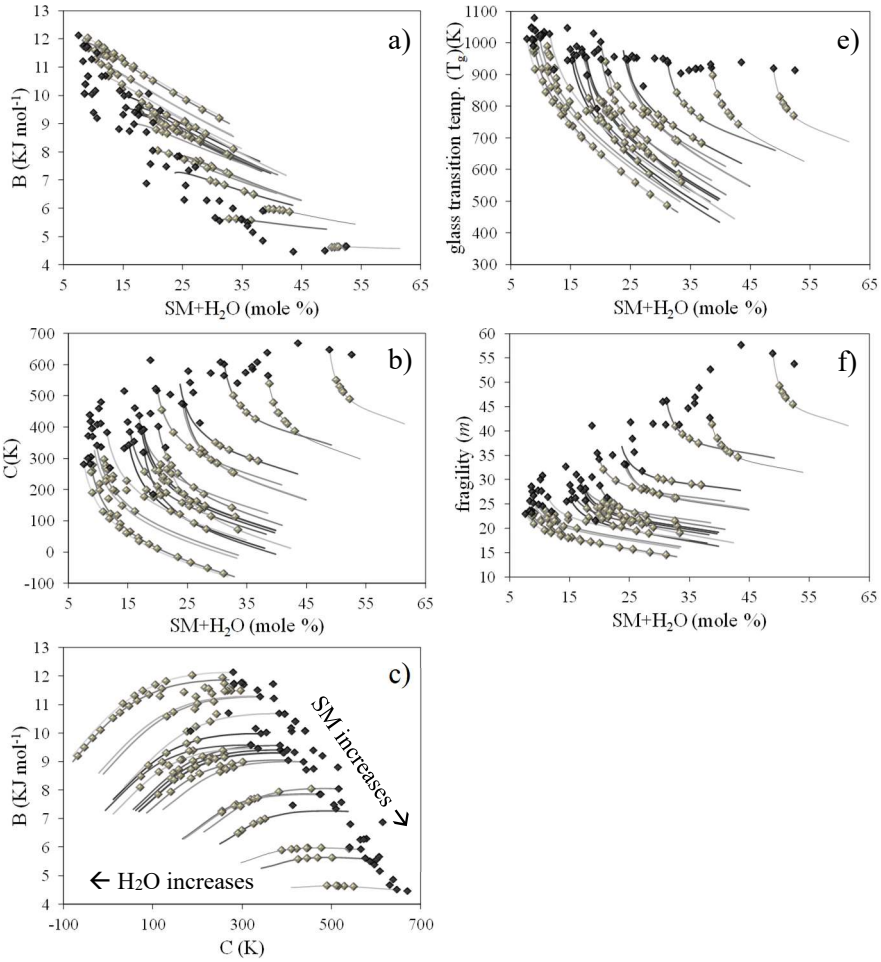

Fig. 2. Relationships between constitutive parameters of the GRD model (Giordano et al., 2008), based on the VFT formulation (Eq. 1), as a function of the modified SM (Structure Modifiers) parameter (Giordano and Dingwell, 2003). The role of increasing SM on the constitutive parameters of anhydrous melts (black symbols) is that of decreasing B_{VFT} and increasing C_{VFT} (Fig. 2a, b) while increasing the fragility (m)(Fig. 2f). On the other hand adding H_2O to the melt structure (gray symbols) results in decreasing B_{VFT} while decreasing C_{VFT}, the glass transition temperature Tg (as taken at a viscosity of 10^{12} Pas)(Fig. 2e) and the fragility (m). This observation put in evidence that the structural role of H_2O is different from that of those cations which simply modify silicate melts structure (Giordano et al., 2008, 2009).

2.2. P – dependent models for predicting melt viscosity.

Measuring the effect of pressure (P) on the viscosity of melts is a complex experimental task and, as a result, has not been investigated extensively. A short summary of applied techniques and technological advances is reported in Appendix A1, together with some of the main results. Largely, the available data imply that the viscosity of silica-rich melts decreases with increasing P, whereas the viscosity of silica-poor melts increases as pressure increases (Liebske et al., 2005; Ardia et al., 2008 and references therein). However, the available data suggest that the effect of P is negligible at near surface conditions pertinent to explosive and effusive volcanism. As a consequence this effect will not be discussed any further in this contribution. Fig. A2.1 shows for

219 the Ab-Di system what is the effect of P which changing composition in the binary system, by using
220 fitting procedure as adopted by Ardia et al. (2008). This system is considered to show what is the
221 effect of P on polymerized (Ab) to depolymerized (Di) synthetic compositions from low to high P.
222 Similar behaviours is expected for natural compositions, but, as shown by previous authors (e.g.
223 Giordano et al., 2008b; Chevrel et al., 2013; Whittington et al., 2009), simplified systems (e.g. An,
224 Di, Ab) should not be considered as proxies for natural compositions.

225

226 ***2.3. Toward a structural model for geological melts.***

227 More recently, Le Losq and Neuville (2017), Giordano and Russell (2018) and Giordano et
228 al. (2019), following different approaches, showed that the viscosity of simple and multicomponent
229 anhydrous silicate melts over a temperature interval of ~ 700 to 1600°C, can be predicted from the
230 Raman spectra obtained from the corresponding glasses (i.e. fast quenched melts). These methods
231 prove to be very promising methods for in situ rheological investigations and may have great
232 importance for planetary sciences studies (Angel et al., 2012; Giordano and Russell, 2018). Le Losq
233 and Neuville (2017) developed a 13 - parameters model for melt viscosity in the simple system
234 SiO_2-Na_2O-K_2O which connects the transport and thermodynamic properties of these simple melts
235 explicitly to the structural state of the melt expressed via the abundances of Q^n -species recovered
236 from Raman spectral analysis of the glasses. Giordano and Russell (2018) first and Giordano et al.
237 (2019), lter, the presented a first order model predicting the viscosity of multicomponent natural
238 melts by the employment of the so-called Raman
239 ratio (R) and normalized Raman ratio (R_n) derived by Raman spectra measured on the
240 corresponding glasses as defined by Mercier et al. (2009, 2010). As shown in Fig. 2 a strong
241 relationship exists between B_{VFT} and C_{VFT} parameters and R which allows the viscosity of
242 anhydrous multicomponent natural melts to be predicted with a great accuracy. Although, the model
243 requires expansion to use of the structural information of volatile-bearing melts, it allows accurate

description of the viscosity of anhydrous melts by the employment of a simple equation with 6 adjustable parameters and the measured R. Also the SM and NBO/T parameters, calculated from compositions, are shown to be strongly correlated with R.

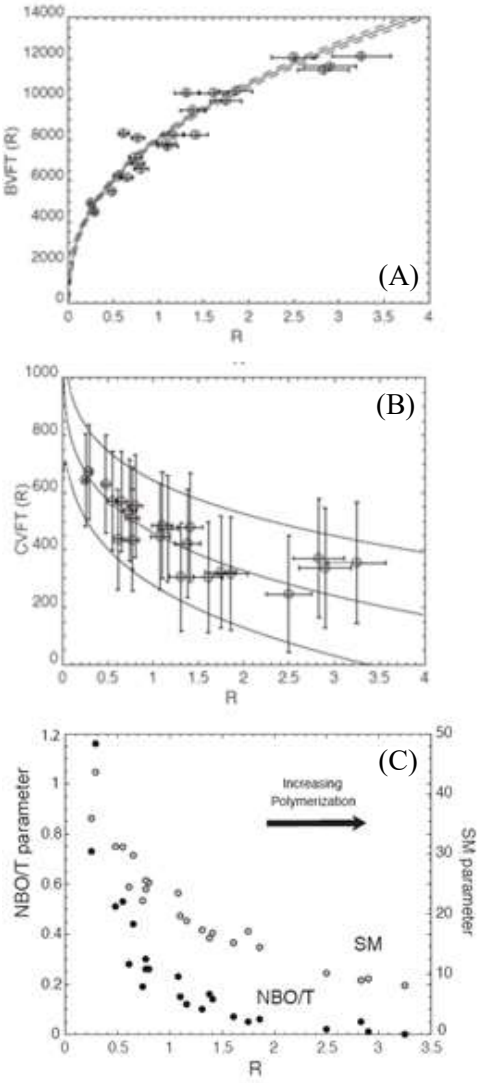

Fig. 2. Model VFT parameters B_{VFT} (R)(A) *and C_{VFT} (R)*(B) *as defined by Giordano and Russell (2018) (panels A, B) and relationships between pseudo-structural parameters (SM, NBO/T)(C), as a function of the Raman ratio (R). According to the above mentioned authors: B_{VFT} (R) = b_1R^{b2} and C_{VFT} (R)=$c_1R^{c2}+c_3$* where *b_1, b_2, c_1, c_2, c_3 are adjustable parameters.*

3. From pure liquids to multiphase analogues and magmas: advantages and disadvantages of the different experimental approaches.

Being magmas and volcanic materials very complex mixtures of crystals and vesicles suspended in a silicate melt phase which evolve as a function of the evolving P, T and compositional variations and dynamic regimes, the description of effect of suspended phases on the

viscosity of these natural suspensions has followed different approaches. The early models devoted to describe the multiphase rheology were historically based on the investigation of analogue materials (e.g. Einstein, 1906; Einstein and Roscoe, 1952). More recently, the basis for the description of natural multiphase suspensions has been largely developed using natural and simplified silicate melts mixtures at experimental conditions at around thermodynamic equilibrium (e.g. Campagnola et al. 2016; Chevrel et al. 2015; Robert et al. 2014; Sehlke et al. 2014; Soldati et al. 2016; Vona and Romano 2013; Vona et al. 2011, 2013). As such, their application to natural environments requires extrapolation into the thermal and deformational disequilibrium state at which magmatic and volcanic processes commonly operate. This is only possible to a limited extent, as natural magmatic and volcanic processes often operate quite far from equilibrium. Recent studies on the disequilibrium rheology of crystallizing natural silicate melts have documented that deformation-rate and cooling-rate may significantly affect the phase transitions of magmatic mixtures so to forcing the material toward a thermal and mechanical disequilibrium state (e.g. Giordano et al., 2007; Kolzenburg et al., 2016, 2017a, b; 2018a,b; Arzilli and Carroll, 2013).

Following, the experimental efforts aimed at retrieving information of the multiphase rheology of natural silicate mixtures have been broadly summarized by subdividing it into, experiments on non reactive materials (chapter 4) or reactive silicate melts mixtures undergoing variable thermal or deformational variation (chapter 5). These kind of experiments can be further subdivided into three main categories: a) experimentation on analogue materials; b) experiments on simplified silicate mixtures and c) experiments on natural volcanic products. Each of these experimental approaches has different advantages/disadvantages which are listed below.

3.1. Analogue materials

Multiphase analogue materials are commonly constituted by non-reactive mixtures of mono- or poly-disperse particles and/or bubbles, with varying content and shape and size distributions,

283 immersed in some Newtonian synthetic fluid (e.g. silicon oil, syrup, liquid paraffin), which can be
284 investigated at room temperature. These kinds of multiphase mixtures can normally be investigated
285 at room temperature conditions and therefore their rheological characterization is simplified as it
286 does not involve the need for high temperature or pressure equipment and the sample texture can
287 readily be controlled (e.g. the solid/bubble proportion or variation). These kinds of experiments are
288 commonly performed on transparent multiphase mixtures and therefore allow observing and
289 characterizing strain partitioning processes occurring amongst the phases during the deformation.
290 The main disadvantage of this kind of experimentation is that they cannot reproduce neither the
291 transient disequilibrium processes occurring in natural mixtures (e.g. crystallization or degassing
292 stages) nor the natural dynamic physical properties of silicate melts (e.g. viscous and cohesive
293 forces between the natural residual melt and suspended particles and bubbles). The largest part of
294 these studies investigate two phase suspensions of either liquid and solid particles (simulating
295 crystal bearing magma) or liquid and bubbles or vesicles (simulating the exsolution of volatile
296 gases).

297

298 ***3.2. Multiphase silicate melt suspensions***

299 The experiments of categories b) and c) require significantly more complex experimental
300 infrastructure and are substantially more complex to be characterized in terms of textural
301 parameters (crystal and bubble content; crystals and bubbles size and shape distributions) but they
302 offer the opportunity to perform measurements on materials with direct application to the Earth
303 Sciences. The inherent inhomogeneity of geo-materials and the large variations of the size– and
304 shape-distributions found in natural products can, to date, not be captured in a satisfactory manner
305 by the available theoretical or empirical models. Experiments on natural materials at controlled
306 conditions have the advantage of being representative of natural scenarios and, in most cases, they
307 allow retrieving, at least, the final stage of textural evolution as a function of the imposed

environmental conditions (i.e. isothermal; non-isothermal; isobaric; non-isobaric) as well as varying deformation regimes (i.e. constant or varying stress and/or strain rate). This allows the reconstruction of the rheological parameters in a tightly constrained parameter space, however it requires unique experimental characterization for each studied scenario. When volatile free samples are investigated, this kind of experiments can be performed, using a variety of experimental techniques (e.g. rotational concentric cylinder/Patterson deformation rig and uniaxial compression and/or micropenetration and parallel plates techniques; see Appendix A1 for details), over the entire temperature-viscosity interval from super- to sub-liquidus conditions that are characteristic of natural environments. For volatile-bearing natural melts and suspensions, this becomes more complex as limited experimental infrastructures exist to date to measure at the elevated pressures required to maintain volatiles in solution. There have been some recent advances which take advantage of the metastable liquid state close to T_g or by using devices which allow the sample to be pressurized (Paterson, 1978; Paterson and Olgaard, 2000; Caricchi et al., 2007; 2008; Ardia et al., 2008; Robert et al., 2008a, b; Piermarini et al., 1978). A further advancement is the 4D characterization of the sub liquidus evolution of natural melts is represented by experiments within synchrotron facilities which allow real time monitoring of the textural evolution of samples of volcanological interest during crystallization and/or degassing (e.g. Ohtani et al. 2005; Pistone et al. 2015; Pleše et al. 2018; Polacci et al. 2018; Polacci et al. 2010; Song et al. 2001). These techniques are starting to be coupled with devices for rheometry, which may in the future allow for in situ measurements of both the crystallization kinetics and the rheological response of evolving natural systems (Coats et al. 2017; Dobson et al. 2015; Dobson et al. 2016; Raterron and Merkel 2009). The results on experimental campaigns and modelling of the multiphase rheology of natural magmatic suspensions performed on natural or analogue silicate melts at high temperatures will be presented in § 4.2.

4. **Experiments and models of non-reactive multiphase mixtures**

Following the results obtained on isothermal bubble-bearing or particle-bearing suspensions rheology of analogue materials, simplified silicate melt mixtures and natural melts and magmas are here first introduced. Finally I summarize what is known on the effect of the presence of bubbles+crystals on suspension rheology measurements performed at constant temperature.

4.1. Models of bubble suspension rheology

Early studies estimating the effect of void spaces within natural and simplified silicate melts (e.g. Bagdassarov and Dingwell1992, 1993; Lejeunne et al. 1999; Vona et al., 2016; Ryan et al., 2019) or synthetic analogues (e.g. Manga et al., 1998; Llewellin et al. 2002a, b; Llewellin and Manga, 2005) has been carried out by several authors. Those investigations showed, largely, that, two end member cases can be considered: 1) bubbles behave as rigid objects (capillary number Ca<1); 2) bubble are deformed (Ca>1)(Llewellin et al., 2002a,b). For the different regimes various empirical equations were proposed (Bagdassarov and Dingwell., 1992; Lejeunne et al.,1999; Llewellin et al., 2002; Llewellin and Manga, 2005)(details in Appendix A3) which suggested, that during steady flow: a) an increase in relative viscosity in the case of the first end-member (Ca<1) and b) a decrease of the relative viscosity in the case of second end member condition (Ca>1) can be observed. Additional complexities are introduced, as discussed in Appendix A3, for non-steady flow for which the definition of a dynamic capillary number (Cd) is required. The same authors (e.g. Lejeune and Richet, 1996; Bagdassarov and Pinkerton, 2004, Llewellin et al., 2002, Llewellin and Manga, 2005) also provided important attainments concerning the understanding of the effect of closed and opened voids on liquid viscosity (e.g. Lejeune et al., 1999; Bagdassarov and Dingwell, 1992; Quane and Russell, 2004; Llewellin et al., 2002a, b; Llewellin and Manga, 2005; Mader et al., 2013; Vona et al., 2016; Ryan et al., 2019). A summary of recent formulations and

works related to both crystal bearing and bubble bearing rheological studies is reported in Appendix A3.

4.2. From shear-rate independent to shear-rate dependent particle suspension rheology models of analogue materials

Early studies on the rheological behavior of multiphase suspensions (e.g. Einstein, 1906; Roscoe, 1952; Krieger and Dougherty, 1959; Gay et al., 1969; Pinkerton and Stevenson, 1992) suggested a threshold in solid fraction, the so-called crystal maximum packing fraction (ϕ_c), that separates a liquid dominated rheology from a solid-dominated rheology. For dilute suspensions of solid mono-disperse spherical particles (ϕ < 3 vol%) Einstein (1906) proposed that the relative viscosity η_r (i.e. the ratio between the viscosity of the particle-bearing suspension and that of the particule-free melts) could be calculated as: $\eta_r = (1 + B\phi)$, where B is a constant depending on object geometrical features (B=2.5 for spheres). Roscoe (1952) extended Einstein's expression to higher concentration of spheres, by first defining the maximum crystal packing fraction (ϕ_m) and providing for the relative viscosity the following expression: $\eta_r = (1+\phi/\phi_m)^{-2.5}$. Different ϕ_m values were proposed by different authors depending on crystal geometry (see appendix A3 for more details). Later, Krieger and Daugherty (1959) generalized the previous expressions as it follows: $\eta_r = (1+\phi/\phi_m)^{-.B e \phi m}$ where B_e is a constant called the Einstein coefficient (KD model). Others similar expressions were formulated for which different value of the B_e coefficients were determined (see appendix A3). Although widely applied, a limitation of those empirical or semi-empirical laws is that they do not account for neither the strain-rate dependence nor the existence of, although still debated, yield strength (Moitra and Gonnermann, 2015) of multiphase mixtures typical of non-Newtonian fluid (see appendix A3 for more details). For a review on the two phase rheology of particle bearing analogue suspensions the reader can refer to Mader et al. (2013), who presented a comprehensive review on this topic.

4.3. Non-Newtonian models for particle suspension rheology of simplified silicate mixtures

Concerning magma-equivalent suspensions, more recently Caricchi et al. (2007), Costa et al. (2007a, 2009), based on the available experimental data obtained at constant temperature, presented models describing the non-Newtonian strain-rate-dependent rheological effects of crystals in the range of solid fractions from 0 to 0.8 and over. These models cover the transition from the regime where the deformation behavior is controlled by melt viscosity up to the beginning of the regime where the deformation behavior is controlled by a solid framework of interlocking particles. The most detailed and comprehensive model to date proposed by Costa et al. (2009) model (CM) (Eqs. A3.3-A3.4.), describes the relative viscosity η_r (i.e. the viscosity of a crystal melt mixture (η_{mix}) divided by the viscosity of the melt phase (η_l)). The CM model is the result of the combined mathematical and experimental efforts condensed in the works of Costa (2005), Costa et al. (2007a) that was used by Caricchi et al (2007) to describe their experimental data. Compared to previous models (e.g., Einstein-Roscoe, 1952; Costa, 2005; Caricchi et al., 2007a), the CM model accounts for the strain-rate dependent changes in the rheology of liquid+crystal mixtures. The model in particular shows that the strain rate dependence of the relative viscosity at varying crystal volume fractions follows a sigmoid curve with exponential increase above a critical solid fraction ($\phi_c \sim 0.3$-0.4). This model is consistent with the early Einstein-Roscoe equation (Einstein, 1906; Roscoe, 1952) for crystal fractions in the range of 0 to 0.1-0.3 depending on crystal shape and size (e.g. Cimarelli et al., 2011). A summary of the main results obtained by the employment of the CM and a summary of its original formulation are reported in Appendix A3. Extension of CM devoted to characterize the effect of crystal size and shape distribution and suspended particle ratio and particle roughness are discussed in Appendix A3.

406 ***4.4. Non-Newtonian strain-rate dependent models for particle suspension rheology of***
407 ***natural mixtures.***

408 The fermenting production of studies (Shaw et al., 1968; Lejeune and Richet, 1995;
409 Giordano et al., 2007; Caricchi et al., 2007, 2008; Ishibashi, 2009; Vetere et al., 2010, 2017; Vona
410 et al., 2011; Pistone et al., 2012, 2016; Chevrel et al., 2015, 2017; Campagnola et al., 2016) devoted
411 to the characterization of the isothermal viscosity evolution of silicate melts at subliquidus
412 temperature as a function of presence and size and shape distributions of crystals and bubbles and
413 deformation regimes of the last twenty years has permitted extraordinary advances that are
414 condensed in empirical and theoretical models of suspension rheology (Saar et al., 2001; Caricchi et
415 al., 2007; Costa et al., 2009; Mueller et al. 2011; Vona et al., 2011; Moitra and Gonnermann, 2015).
416 According to the comprehensive model of Costa et al (2009)(CM)(see § 3.1), inspired by the
417 previous work of Costa (2005), Costa et al. (2007a) and Caricchi et al (2007), the relative viscosity
418 of two-phase mixture increases following a sigmoid curve with exponential increase above a critical
419 solid fraction (ϕ_c) corresponding to the first (phi~0.3-0.4) inflection point. A second inflection point
420 (ϕ_m) at phi ~0.6-0.7 is determined by the beginning of crystal dominated rheology (Fig. A3.3).

421 Since the seminal contributions of Caricchi et al. (2007) and Costa et al. (2009), numerous
422 scientists provided new and more complete formulation of the critical crystal fraction (ϕ_c) for the
423 natural variability in of crystal size and shape distribution which would also account for new
424 variables (e.g. crystal surface roughness)(e.g. Mueller et al. 2011; Klein et al., 2018). The
425 employment of these critical contributions have allowed interpreting, based on model calculations,
426 the effect of rheological constraints on eruptive behavior.

427

428 ***4.5. Models for particles and bubbles suspension rheology***

Complex three-phase suspensions (i.e. liquid+bubbles+crystals) have been investigated in only a few studies (Cordonnier et al., 2009; Robert et al., 2008a, b; Lavalleé et al., 2007, 2008; Vona et al., 2013, 2017; Campagnola et al., 2016; Pistone et al., 2012, 2015, 2016). Given their complexity only a fewer studies have provided preliminary models describing the complex rheology of three-phase mixtures (Pistone et al., 2012, 2013, 2015, 2016). The viscosity data presented in those studies are the same as those presented in Pistone et al (2012), but the authors apply their results to different geological context by showing that size- and shape-distributions of crystals and bubbles may significantly vary while undergoing certain stress-strain regimes. The experiments by Pistone et al. (2012) were performed at pressurized and isothermal temperature conditions in a Paterson device (Appendix A1) on samples for which the liquid+crystal rheology was characterized by Caricchi et al. (2007). They show that bubbles strongly affect the rheological properties of crystal-rich mushes. By presenting a comprehensive review of existing literature and performing new measurements, they estimated that a decrease of up to 4 orders of magnitude is observed by the addition of only 9 vol% of bubbles to a liquid+crystals suspension containing 70 vol% of crystals. They also established that two non-Newtonian deformation regimes originate as a consequence of the bubble and crystal interaction: i) a shear thinning behavior result of the crystal size reduction and shear banding due to strain localization (also observed by Caricchi et al. 2008) which is typical of magmas which are transported and emplaced in Earth's crust and may feed eruptions; ii) a shear thickening behavior which is the consequence of crystal interlock and flow blockage which they argue locks plutonic rocks in the lower and upper crust, inhibiting eruptions. More details of the results obtained by the works of Pistone and coauthors are provided in Appendix A3.3.

5. Non-Isothermal cooling-rate and strain-rate dependent rheology of volcanic materials

Efforts to systematically describe and predict magma migration and lava flow behavior rely heavily on these experimental measurements to derive empirical models. However, during migration and transport of silicate melts in the Earth's crust and at its surface magma/lava can experience varying cooling and deformation conditions which may drastically influence its thermorheological evolution; see for example Rhéty et al. (2017) and Robert et al. (2014). As a consequence, data intended for application to the natural environment will have to account for the disequilibrium behavior of natural magmatic suspensions. Cooling rates of basaltic lavas, measured at the surface and within active lava channels during emplacement range from ~0.01 to 15 ℃/min (Cashman et al., 1999; Flynn and Mouginis-Mark, 1992; Hon et al., 1994; Witter and Harris, 2007; Kolzenburg et al., 2017). These values are largely representative for the exterior part of lava flows or for the initial cooling of newly emplaced dikes. They can, therefore, be taken as maximum cooling rates that are expected to be lower in the interior of the lava flow or a cooling dike. The importance of varying thermal conditions on the crystallization kinetics and textural development of silicate melts has been recognized for decades and inspired disequilibrium experimentation in petrology and volcanology (e.g. Walker et al., 1976; Arzilli and Carroll, 2013; Coish and Taylor, 1979; Gamble and Taylor, 1980; Hammer, 2006; Lofgren, 1980; Long and Wood, 1986; Pinkerton and Sparks, 1978; Giordano et al., 2007; Vetere et al., 2013). These studies highlight that significant differences in textures and paragenesis emerge when moving from equilibrium to disequilibrium conditions that can, in turn, affect the flow behavior. Albeit a growing experimental disequilibrium database is becoming available no models for the disequilibrium phase dynamics of natural silicate melts have been developed to date.

Understanding the rheological evolution of crystallizing melts, magmas and volcanic products requires direct measurement of the flow properties of investigated materials at such disequilibrium conditions in the field or in the laboratory. In such environments, the studied materials are degassed and undergoes transient increases in viscosity as it is increasingly

undercooling until a “rheological cut-off temperature” (Giordano et al., 2007, Kolzenburg et al., 2016, 2017, 2018a, b, c; 2019) is reached and the lava rheologically solidifies. This transient rheological gradient, which occurs in all natural, non-isothermal environments, governs the lavas emplacement style. In recent years, the first sets of measurements were presented that constrain the rheological evolution of natural silicate melts under temperature- and deformation-conditions pertinent to the transport of silicate melts on the earth’s surface and in shallow magma plumbing systems. The recovered data show a strong dependence of composition (Kolzenburg et al., 2017, 2018a), cooling-rate (Giordano et al., 2007, Kolzenburg et al., 2016, 2017), oxygen fugacity (Kolzenburg et al., 2018a) and shear-rate (Kolzenburg et al., 2018) on the thermorheological evolution of natural silicate melts. They represent the first contributions to a growing database of lava rheology under natural conditions. However, significant experimental effort in this field is required to expand the range of available data to cover the most relevant compositions and to experimentally map the range of parameters pertinent to flow of natural silicate melts under disequilibrium. Such a database would then allow deducing the underlying processess and expanding these into a theoretical description of the flow behavior of magma and lava. So far, the main limitation of these kind of studies is the difficulty to monitor, and therefore extend, the results to non-degassed materials and therefore the application to intra-crustal magmatic or explosive volcanic processes. According to previous authors (e.g. Melnik and Sparks, 1999, 2005; Costa and Macedonio, 2003, 2005; Costa et al., 2007b; Hess et al., 2008; Cordonnier et al., 2012) an additional complexity could be due to the effects of nonlinear thermal effects, potentially generated by viscous dissipation and loss by conduction at the contact between the molten material and the hosting rock, in conduits, and channels or tunnels after eruption to the surface. The nonlinear behaviour of thermal effect are mainly governed by specific non-dimensional numbers (Graetz; Nahme; Prandtl; Reynolds; regime), which according to Costa et al. (2007b), amongst the others above mentioned, may determine the necessity to distinguish between three main regimes - a conductive-heat-loss-dominated regime, an intermediate regime and a viscous-heating-dominated -

505 may have significant effects for the definition of the rheological behaviour and emplacement
506 dynamics of lava flows and lava domes.

507 Figure 3 shows a summary of rheological data recovered using a variety of experimental
508 methods on Etna melts. The melt compositions, albeit stemming from different eruptions, are
509 similar for most major oxides with the exception of the sample from Vona et al. (2017), that is more
510 rich in silica and poor in iron and, as a result, more viscous than the samples in Vona et al. (2011)
511 and Kolzenburg (2018).

512 For the investigated degassed materials these data summary highlights a number of effects
513 acting during the transport of magma and lava at sub liquidus conditions. Comparison of the pure
514 liquid viscosity of the remelted bulk rock and the separated groundmass (Vona et al., 2017); open
515 triangles documents that, for basaltic melts, crystallization induced changes in melt composition
516 result in relatively small changes in the viscosity of the liquid phase of the evolving suspension.

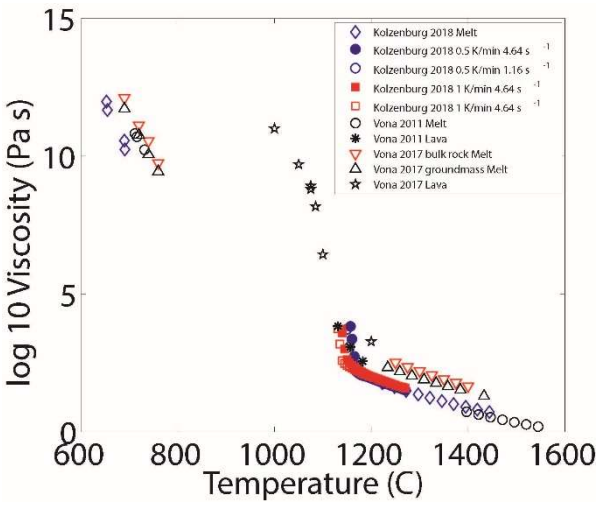

517
518
519 *Fig. 3. Summary of available melt and crystal-suspension viscosity data on remelted Etnean lava as a function*
520 *of temperature. Melt viscosity measurements (open blue diamonds, black circles and black and red triangles) were*
521 *performed via concentric cylinder viscometry, micro penetration and differential scanning calorimetry; Sub liquidus*
522 *viscosity measurements were preformed using 1) concentric cylinder viscometry at constant temperature (black plus*
523 *symbols), 2) concentric cylinder viscometry at varying cooling- and shear-rates (open and filled red squared and blue*
524 *circles) and 3) parallel plate viscometry via unconfined uniaxial deformation (open black stars).*
525
526 Therefore, the variations of the flow behavior of crystallizing basalts are controlled by
527 variations in the volumetric fractions of crystals and bubbles. These data also reflect the

528 measurement limits of the respective methods that are described in more detail in Kolzenburg et al.
529 (2016a). Concentric cylinder suspension viscometry for these Etnean lavas is confined to $<10^4$ Pa s
530 and shows that the measured viscosities at constant temperature (i.e. at or near thermodynamic and
531 textural equilibrium) are commonly higher than non-isothermal measurements at the same
532 temperature. This is due to the fact that under dynamic thermal conditions, the crystal nucleation
533 and growth kinetics lag behind the equilibrium state and commonly produce lower crystal contents.
534 The non-isothermal viscosity data from Kolzenburg et al. (2018c) document that both cooling-rate
535 (blue circles vs. red squares) and shear rate (open vs. filled symbols) exert a modulating effect on
536 the disequilibrium rheology of the Etna melt. Measurements beyond the mechanical limit of
537 concentric cylinder (CC) viscometry were presented in Vona et al. (2017) who employed parallel
538 plate (PP) viscometry via unconfined uniaxial deformation (open black stars) to measure the
539 viscosity of three phase magmatic suspensions. The data form an apparent continuing trend with
540 respect to the concentric cylinder viscometry measurements but document lower lava viscosities
541 than extrapolation from the two phase measurements would suggest. This is likely a result of the
542 differences in sample texture, where all CC data are restricted to bubble free two phase suspensions
543 of crystals and melt, whereas the PP data are measured on three phase (i.e. crystal and bubble
544 bearing) suspensions.

545 In summary, the rheological evolution of lava at sub-liquidus conditions can be
546 reconstructed neatly by combination of datasets from differing sources. This is also shown in Figure
547 3 in Kolzenburg et al., 2019 (this issue), where laboratory and field estimates of lava rheology at
548 emplacement conditions are compared and the respective data fall within a range of similar values.
549 This highlights the potential of cross correlation of data from different experimental and field
550 sources and the need to expand the available experimental database in order to generate a holistic
551 view of the dynamics of magma and lava transport.

552

6. Alternative ways of retrieving rheological information from remote sensing ground- or satellite-based techniques.

Besides laboratory viscometry (i.e. the direct measurement of melt / suspension viscosity under controlled conditions) there are several other sources of rheological information that are useful to place the laboratory measurements in context of the natural environment. This kind of information is important as it allows accounting for the multiphase nature of lava bodies and can serve to place the laboratory measurements within the framework of conditions relevant in natural scenarios. However, to date such data only represents a very limited source of information of the rheological evolution of lava flows, in space and time. This is largely due to large logistical and financial efforts required for some of these measurements and the uncertainties associated to others. Broadly these approaches can be separated into:

1. Direct measurement of viscosity on active lava flows via penetration- or rotational-viscometry (Einarsson, 1949; Gauthier 1973; Panov et al. 1988; Pinkerton and Sparks, 1978; Belousov et al. 2015; Belousov and Belousova, 2018; Shaw et al., 1968; Pinkerton and Norton, 1995; Pinkerton and Wilson, 1994; Chevrel et al., 2018). These represent snapshots of actual lava flow rheology at specific conditions and provide data that helps to constrain the conditions required to be reproduced in systematic laboratory studies. However, such measurements are quite difficult and require significant logistical effort and manpower. Further, the available devices (e.g. Belousov and Belousova, 2018; Chevrel et al., 2018) for such measurements are only slowly advancing to be able to measure all relevant parameters sufficiently well to recover high quality viscosity data (Appendix, A1.5).
2. Calculation of the apparent viscosity based on Jeffreys' equations (e.g. Jeffrey, 1925; Hulme, 1974)(Appendix 4, SMO) using flow rate measurements of active lavas in channelized flows (Naboko 1938; Nichols 1939; Minakami 1951; Einarsson 1966; Walker 1967; Gautier 1973; Moore 1978; Andreev 1978; Fink and Zimbelman 1986; Vande-Kirkov 1987; Panov 1988;

578 Soldati 2016; Belusov and Belousova 2018). Such data are still few due to the difficulty of
579 accessing active lava flows. However, the development of affordable unmanned aerial
580 vehicles (UAV's) in recent years appears to be promising making this method widely
581 applicable with the opportune considerations. In fact, the above mentioned approach has
582 strong limitations as it is based on the assumption of parabolic velocity profile that is not
583 generally valid because of thermal effects (e.g. Costa and Macedonio, 2003, 2005; Costa et
584 al., 2007b; Filippucci et al., 2013 and Filippucci et al., 2019, this issue)(details at § 3.1.2).
585 Such aspect is still never considered to describe the nonlinear dynamic of lava flows and lava
586 domes rheology (Melnik and Sparks, 1999, 2005; Melnik et al., 2009). To an adequate
587 analysis of this contribution for specific cases, it is recommended to refer, for instance, to the
588 above mentioned works and e.g. Filippucci et al (2019)(this issue).
589 3. Ties between lava flow geometry and viscosity. Morphological-derived rheological
590 parameters (i.e. viscosity and yield strength) are commonly obtained in planetary sciences
591 (Heisinger et al., 2007; Castruccio et al., 2010 and Chevrel et al., 2015 provide excellent
592 reviews of the employed equations and results). Rheological information is obtained by
593 retrieving, in the field or remotely also from satellites, length, width, thickness and slope of
594 emplacement of lava flows. This methodology has also been applied based remote sensing
595 data collected during active flow emplacement (James et al., 2015, Farquarson et al., 2015;
596 Kolzenburg et al., 2018a). Also in this case, the emplacement of lava flows is commonly
597 modelled using a single rheological parameter (apparent viscosity or apparent yield strength)
598 calculated from morphological dimensions using Jeffreys' and Hulme's (Jeffrey and Acrivos,
599 1976; Hulme, 1974) equations. The rheological parameters are then typically further
600 interpreted in terms of the nature and chemical composition of the lava (e.g., mafic or felsic).
601 Chevrel et al. (2013, 2015) employing this methodology has shown that providing an unique
602 factor to describe rheology of lava flows is definitely far from being representative of the real
603 emplacement dynamics of lava flows. As above mentioned (point 2), given the nonlinear

dynamics of lava flows and domes, which may determine significant thermal effects, significant limitations may be observed and should be carefully considered before applying to any natural context (e.g. Costa and Macedonio, 2003, 2005; Costa et al., 2007b; Filippucci et al., 2013 and Filippucci et al., 2019, this issue).

4. Ties between the intensity of thermal anomalies generated by actively flowing lava and its silica content and therewith discharge rate of lavas (e.g. Coppola et al., 2013, 2017). This approach takes advantage of the fact that low viscosity lavas are readily able to spread into thin sheets during flow, whereas high viscosity lavas usually retain lower aspect ratios. Since the heat loss of a lava is largely governed by its surface to volume ratio, its spreading ability (i.e. viscosity) can, empirically, be correlated to the measured heat loss. Over the last decades such satellite-based remote sensing and data processing techniques have proved well suited to complement field observations and to allow timely eruption detection, as well as for flow tracking.

7. Concluding remarks and outlook

The present review shows the extraordinary improved knowledge of rheological properties of multicomponent and multiphase silicate melts occurring in the last twenty years. Such knowledge advancement has been due to the necessity of constraining natural processes and parallel the development of new technological advances, frequently obtained to face specific problems. It has been observed that the continuously evolving rheology of magmas and eruptive products during their ascent, eruption and emplacement can be described with increasing accuracy and specifically applied to geological issues with improved confidence. The observed transition between Newtonian to strongly non-Newtonian rheological behaviour is typical of both simple liquids and/or multiphase natural mixtures. These transitions govern the observed eruption dynamics and the eruption dynamic transitions, potentially determining also whether an eruption will be effusive or explosive.

629 The employment of the rheological flow laws for multicomponent and multiphase silicate
630 melts find a very promising application to constraining the advancement and halting of lava flows.
631 For these superficial phenomena, the opportunity of monitoring important variables such as the
632 discharge rate and the topography of emplacement provide fundamental advantage for the
633 employment of numerical simulations tools. These have allowed showing that more accurate
634 estimates of the effects of crystals and bubbles during lava flow emplacement can be obtained only
635 by real-time monitoring of lava flows through field and remote sensing methods paralleled by a
636 proper experimental campaign, which in particular would account for the non-equilibrium, non-
637 isothermal rheology of multiphase mixtures.

638 This progress in understanding the mechanisms of advancement and emplacement of lava
639 flows and domes has also been made possible recently thanks to the recent emplacement of large
640 long-lasting silicic to basaltic effusive eruptions. Prior to 2008, for instance, no rhyolite lava flow-
641 forming eruptive event was observed or documented. Hence, the real-time observations of active
642 rhyolitic flow and dome emplacement at the Chilean volcanoes of Chaitén (Carn et al. 2009; Lara
643 2009; Bernstein et al. 2013; Pallister et al. 2013) and Puyehue-Cordón Caulle significantly
644 developed our knowledge of rhyolitic lava emplacement (Castro et al. 2013; Schipper et al. 2013;
645 Tuffen et al. 2013; Bertin et al. 2015; Farquharson et al. 2015; Magnall et al. 2017). Analogously
646 the long lasting 2014-2015 basaltic eruption at Holuhraun, Bardarbunga system, Iceland (e.g.
647 Pedersen et al., 2017), offered the opportunity to establish/calibrate, through the contemporaneous
648 employment of field work, remote sensing techniques (Kolzenburg et al., 2018a) and laboratory
649 experimentation (Kolzenburg et al., 2017), which allow retrieving thermal properties, estimates of
650 effusion rate (Coppola et al., 2013, 2017) and evaluate the effect of bubbles by comparison with
651 experimental campaign on liquid+ crystals material as collected during eruption (Kolzenburg et al.,
652 2017, 2018a,b). Worth mentioning is also the integrated field, remote sensing, physical properties
653 and physical modelling and numerical simulations studies performed in the recent years for

654 intermediate compositions producing effusive activities (Chevrel et al., 2013a,b; 2015). For
655 andesitic domes huge progresses in understanding the non-linear thermal effects which determine
656 non-linear eruption dynamics has been made by previous authors (e.g. Costa et al., 2007b; Melnik
657 and Sparks, 1999, 2005; Melnik et al., 2009). Although the purposes of this paper is to mostly
658 describe the development of rheological properties in relationship to the emplacement of lavas,
659 most of the general results obtained here, and in particular those related to the effect of crystals and
660 vesicle on multiphase rheology, can be extended to eruption dynamics of explosive phases.

661 Some of the main results deduced by application of the existing rheological models and
662 experimental studies, supported by petrological analysis and field work, allowed to unequivocally
663 show that lava flow emplacement may be a long lasting process also for silicic magmas and that
664 flow may continued also unrooted from the vent for long times (e.g. Farquarson et al., 2015) and
665 that extremely voluminous silicic lava flows may be emplaced in relatively short time without
666 giving origin to significant explosive stages (Tuffen et al., 2013; Farquarson et al., 2015; Giordano
667 et al., 2017; Polo et al., 2018a, b). In addition, Kolzenburg et al (2016, 2017, 2018) showed that
668 disequilibrium, cooling- and shear-rate controlled rheological properties may have fundamental
669 influence in determining the effective length of basaltic lava flows.

670 Although the results evidenced by performing non-equilibrium, non-isothermal, transient
671 rheology of basaltic lava flows, are promising and provided a first understanding of lava flow
672 rheology under natural conditions, it is possible to anticipate that future studies will require
673 performing this kind of experiments also to a wider range of effusive products.

674

675 **Acknowledgements**

676 I would like to thank Stephan Kolzenburg and Kelly Russell for sharing ideas and help in
677 the reorganization of the manuscript. Fabio Arzilli and an anonymous reviewer are also

678 acknowledged for the careful revision of the manuscript. Daniele Giordano acknowledges the
679 University of Turin for support provided by local research funds (2017/2020).

680

681 **APPENDICES**

682 **Appendix A1. Short review of some of the most common methods to measure viscosity.**

683 The basic nature of magmas and volcanic products changes from liquids, through foams,
684 emulsions, crystal suspensions, and partially molten aggregates. The rheology of such widely
685 varying materials, each complex in its own right, and the fact that the viscosity of these materials
686 can span over, at least, 16 orders of magnitude, defies the use of one single method to fully
687 characterize their behavior. A large variety of devices for the measurement of the deformation and
688 transport behavior of magmas, lavas and other volcanic materials have been presented in literature
689 to date and this continuously evolving field produces novel techniques on a regular basis. These
690 range from new devices for laboratory measurements to novel methods for ground- and satellite-
691 based viscosity estimates. This field is growing in order to accomplish the complex task of defining
692 the rheology of natural systems or analogues.

693 In principle, viscosity information of a material can be obtained from any data where time
694 evolution of strain ($\gamma = (dx/dz)$) and strain-rate $\left(\dot{\gamma} = d\gamma/dt = 1/dt\ (dx/dz)\right)$ in response to an
695 applied stress (σ) can be recorded.

696 Viscometry can therefore be performed in devices where either strain-rate is maintained
697 constant while the resulting stress is measured (e.g., concentric cylinder) or when the imposed stress
698 is kept constant and the resulting strain-rate is measured (e.g., micropenetration and fiber
699 elongation; Dingwell et al., 1993). For the sake of brevity, we will not report the details and
700 analytical procedure of each experimental device here but rather we will provide the most relevant
701 reference papers describing the devices and the experimental procedures in detail.

702 Experimental efforts are to date largely subdivided into two categories of two phase
703 suspension rheometry, namely i) those measuring volatile-bearing suspensions and, ii) those
704 measuring particle bearing suspensions where volatiles cannot be retained dissolved in the liquid
705 phase at experimental conditions. At room temperature conditions this distinction fundamentally

identifies two temperature intervals: i) low-temperature experiments, at or close to the glass transition temperature, where volatile dissolution kinetics and, in most cases, crystals formation processes are slow enough not to allow gas exsolution and crystal formation during the experiment (these span viscosities in the range between ~ 10^8 to 10^{12}) and, ii) the high-temperature experiments, where pure liquid and liquid+crystals measurements can be performed. A small number of laboratory studies of viscous deformation of volatile and crystal-bearing mixtures at high pressure and temperature also exist. The main advantage of these apparata is that they they attain P-T conditions more realistic for geologically relevant multiphase assemblages and they allow measurements on volatile bearing liquids at superliquidus conditions.

A1.1. Rotational (Couette) rheometry

The advantage of the rotational concentric cylinder viscometry, compared to other viscometers, is the possibility to operate continuously at given conditions (e.g. shear rate or shear stress), so that steady-state measurements can performed while systematically varying the experimental conditions. This allows detecting and quantifying any time dependency of the viscosity of the studied material via measurement at different shear rates, temperature, etc. Therefore, rotational viscometers are among the most widely used devices for measurements on magma rheology. The most common type are Searle-type viscometers, where the inner cylinder rotates (at constant strain-rate or stress). The sample is deformed in an annulus of liquid filling the gap between a rotating inner spindle (commonly a cylinder, or a cone-plate geometry) and an outer cylindrical cup. Rheometry on natural silicate melts is commonly performed in a wide gap geometry, where the velocity profile across the deforming liquid or suspension is non-linear. As such, determination of the sample viscosity relies on calibration of the measured torque against well characterized standard materials for which the temperature viscosity relationship is accurately known.

731 Viscosities are calculated from the equation for Newtonian liquids:

732 $$\eta = \frac{M}{4 \cdot \pi \cdot \Omega \cdot (l)} \left(\frac{1}{r^2} - \frac{1}{R^2} \right) \qquad \text{(Eq. A1.1)}$$

733 where M is the torque, Ω is the angular velocity of the outer cylinder, r and R are the respective
734 radii of the inner and outer cylinders, and (l) is the effective length of the inner cylinder.

735 As above mentioned, the common approach for natural silicate melt viscometry at high
736 temperature is to use a wide gap geometry and calibrating the torque exerted on a spindle to the
737 melt viscosity using a standard. As it can be retrieved by Eq. A1.1 wide gap geometry has the
738 disadvantage of being slightly less accurate than small gap geometry, but the advantage of
739 introducing small viscosity reading errors in the case of crystallization on the adopted rotating
740 spindles or in the gap space.

741 Early devices of this type that produced a plethora of experimental data are described in a
742 series of papers measuring the viscosity of synthetic silicate melts (Dingwell 1986; Dingwell 1989;
743 Dingwell and Virgo 1988). For these high temperature rheological experiments a solid precious
744 metal spindle is hung from the measurement head and immersed into the sample while being rotated
745 at a constant rate. In this setup, the torque needed to maintain a constant rotation rate is proportional
746 to the melt/suspension viscosity and is recorded at a frequency of ~1 Hz. The spindles used in these
747 experiments vary in diameter and are chosen depending on the expected melt viscosity, to suit the
748 torque and deformation rate range of interest. They are commonly machined to have a 45° conical
749 top and bottom to reduce edge effects. Calibration of these devices is performed for shear-rates and
750 temperatures exceeding those used in the experiments to account for mechanical effects in the
751 measurement setup. The precision of the viscosity determination is ca. ±3% as described in
752 Dingwell (1986). Since direct temperature measurement during viscometry was not possible up
753 until recently, the thermal evolution of the sample at the imposed temperatures is commonly
754 calibrated over the entire experimental temperature range using a platinum sheathed type-S

thermocouple immersed in an inert standard glass that does not crystallize over the entire calibration range.

The concentric cylinder is used to investigate both volatile-free liquids (at above liquidus conditions) and liquid+crystal suspensions (at subliquidus conditions) over the viscosity range between 10^{-1} and 10^{4} Pa s (Dingwell and Virgo, 1988; Chevrel et al. 2015; Chevrel et al. 2013a; Dingwell 1989; Dingwell and Virgo 1987; Giordano et al. 2005, 2006; Kolzenburg et al. 2016b; 2017; Sato 2005; Vetere et al. 2017; Vona et al. 2011, 2013). It has also been employed to study the effect of changing oxygen fugacity on melt and suspension viscosity via combination with gas mixing furnaces (see for example Dingwell and Virgo,1987, Chevrel et al., 2013a, Kolzenburg et al., 2018b).

There are two dominant mechanical constraints of these experimental apparatuses that inhibit rheometry at high viscosity values presented here 1) the torque limit of the rheometer head and 2) the fact that the crucible containing the experimental sample may start to slip and rotate in its holder at high torque, rendering the measured torque data useless. This issue was addressed recently in the construction of a new rheometer by Morgavi et al. (2015), who designed a new crucible coupling, allowing both viscometry at higher torques, expanding the measurement range to 10^{4} Pa s, and allowing also for chaotic mixing experiments.

A further advancement in concentric cylinder viscometry at sub liquidus conditions was the development of an experimental device and method for in-situ differential thermal analysis during concentric cylinder rheometry as presented in Kolzenburg et al. (2016a). This device allows tracking the crystallization relates change in the effective viscosity of the suspension due to crystallization as well as the latent heat released during crystallization. Such a device, in turn allowed studying the shear rate dependence of sub liquidus lava rheology at conditions pertinent to lava flow emplacement (Kolzenburg et al., 2018c,d).

779

780 ***A1.2. Dilatometric methods***

781 These methods can be used to measure, at close to glass transition temperature (e.g.
782 viscosity between 10^8 and 10^{14} Pa s), pure liquid as well as two-phase and three-phase suspensions
783 (Robert et al., 2008a,b; Vona et al., 2013). The most widely such a devices are the dilatometric
784 method of the micropenetration (Hess and Dingwell, 1986) and the uniaxial parallel plate (e.g.
785 Robert et al., 2008a, b) the details of which are provided below.

786 *Micropenetration*

787 Micropenetration technique involves determining the rate at which an hemispherical Ir-
788 indenter moves into the melt surface under a fixed load. The sample is placed in a silica rod sample
789 holder under an Argon gas flow. The indenter is attached to one end of an alumina rod. The other
790 end of the alumina rod is attached to a mass. The metal connection between the alumina rod and the
791 weight pan acts as the core of a calibrated linear voltage displacement transducer (LVDT)(e.g. Hess
792 and Dingwell, 1996). The movement of this metal core as the indenter is pushed into the melt yields
793 the displacement. The absolute shear viscosity is determined via the following equation
794 (Pocklington, 1940; Tobolsky and Taylor, 1963):

795 $$\eta\ (Pa \cdot s) = \frac{0.1875 \cdot P \cdot t}{r^{0.5} \cdot \alpha^{1.5}} \qquad \text{(Eq. A1.2)}$$

796 where P is the applied force, r is the radius of the hemisphere, t is the penetration time and α
797 is the indentation distance. This provides an accurate viscosity value if the indentation distance is
798 lower than 150 – 200 microns. The technique allows viscosity to be determined at T up to 1100°C
799 in the range $10^{8.5}$ to 10^{12} Pa·s without any problems with vesiculation. One advantage of the
800 micropenetration technique is that it only requires a small amounts of sample (other techniques used
801 for high viscosity measurements, such as parallel plates and fiber elongation methods instead
802 necessitate larger amount of material).

Parallel plate

Using the parallel plate technique, the shear viscosity of the cores is computed for a given applied load (F; N), sample volume (V; m^3), sample length at time t (L; m), and rate of shortening ($\partial L/\partial t$; m/s) using the "no-slip" (Eq. A1.2), and "perfect-slip" (Eq. A1.3) models of Gent (1960) (cf. Dingwell et al. 1993):

$$\eta_S\ (Pa \cdot s) = \frac{2\pi \cdot L^5 F}{3V \cdot \frac{dL}{dt}(2\pi L^3 + V)} \qquad \text{(Eq. A1.3)}$$

and

$$\eta_S\ (Pa \cdot s) = \frac{L^2 F}{3V \cdot \frac{dL}{dt}} \qquad \text{(Eq. A1.4)}$$

respectively. The "no slip" equation is used for the case in which the surface area of contact between the melt and the parallel plates remains constant and the cylinder bulges with increasing deformation. The "perfect slip" equation is used for the case in which the surface area between the cylinder and the plate increases with deformation and the cylinder does not bulge.

A1.3. Falling Sphere method (Simple and centrifuge)

The falling sphere method relies on determining the speed of a sphere (typically made of metal) falling through molten material. Viscosity is calculated according to the Stokes law as it follows:

$$\eta\ (Pa \cdot s) = \frac{2}{9} \cdot \frac{(\rho_S - \rho_M) \cdot a \cdot r^2}{v} \cdot C_F \qquad \text{(Eq. A1.5)}$$

where η is the viscosity (Pa·s), ρ_S-ρ_M the density contrast between the sinking sphere and the melt (kg/m3), a the acceleration of typically 1g (m/s^2), r the radius of the sphere (m), and v the velocity of the sinking sphere (m/s). C_F is the Faxèn correction term (Faxèn, 1922), which accounts for interactions between the sinking sphere and the wall of the capsule expressed by

825 $$C_F = 1 - 2.104 \cdot \left(\frac{r}{R}\right) + 2.09 \cdot \left(\frac{r}{R}\right)^3 - 0.95 \cdot \left(\frac{r}{R}\right)^5 \quad \text{(Eq. A1.6)}$$

826 where R is the radius of the container, in which the sphere is positioned in the center. The
827 Faxèn correction is considered to result in a slight underestimation of the calculated viscosity, but
828 constitutes the best expression to account for the wall-effect on viscosity (Kahle et al., 2003).

829 Maximizing the density contrast (ρ_S - ρ_M) between the sphere and the melt reduces the
830 uncertainty associated with the estimation of melt density. As a consequence Pt (ρ_S=21450 kg/m^3)
831 or Mo spheres (ρ_S=10220 kg/m^3) are commonly employed.

832 Experiments that allow to investigate the variation of viscosity at the P-T-X(H_2O)
833 conditions relevant to magmatic and volcanological environments are incredibly time consuming
834 and require significant experimental effort. The range of viscosities investigated with the falling
835 sphere technique varies from 10^{-4} Pa s (Brearley et al., 1986; Behrens and Schulze, 2003; Audetat
836 and Keppler, 2004; Kanzaki et al., 1987; Taniguchi, 1995; Suzuki et al., 2005) to $10^{4.5}$ Pa s
837 (Kushiro et al., 1976; Kushiro, 1976, 1977, 1978; Baker and Vaillancourt, 1995; Schulze et al.,
838 1999; Liebske et al., 2005; Vetere et al., 2006; Del Gaudio et al., 2007). At the lower viscosity end
839 (<1 Pa s), represented by ultramafic melts, real time movies of the falling sphere are necessary and
840 are obtained through the use of X-rays from a synchrotron source. At the upper viscosity end ($10^{4.5}$
841 Pa s), represented by granitic melts, the sinking distance of the sphere becomes smaller than its
842 diameter and the sum of the experimental errors in determining the sphere location. Falling sphere
843 viscometry has been employed at ambient (Dorfman et al., 1997; Riebling, 1966) and high-P
844 conditions (e.g. Kushiro, 1978; Ryan and Blevins, 1987; Persikov et al., 1990; Scarfe et al., 1986;
845 Dingwell, 1987; Brearley and Montana, 1989; and White and Montana, 1990; Baker and
846 Vaillancourt, 1995; Schulze et al., 1999; Liebske et al., 2005; Vetere et al., 2006; Del Gaudio et al.,
847 2007) within piston cylinders and multi anvils (up to 130 kbar, Liebske et al., 2005) for
848 simultaneous determination of density and viscosity. Maximizing the density contrast between the

falling sphere and the surrounding melt reduces errors associated with the estimation of melt density and viscosity. Errors in density contrast can easily be reduced below the uncertainties inherent in the other variables affecting viscosity determination. Total errors for falling sphere viscosity determinations using the piston cylinder apparatus are probably nearer 20%. Burnham (1963) describes a variant on the falling sphere method in which the fall of a sphere, connected to a wire isolated electrically from the metal capsule, was electrically detected by the contact of the sphere against the capsule wall. Persikov et al. (1990) used a radioactive-tracer doped falling sphere in an internally-heated pressure vessel. The descent of the sphere is recorded radiographically as the sphere transits two "windows" in a lead shield. Very high pressure measurements of viscosity have been made by Kanzaki et al. (1987) who imaged the falling sphere in real time using a synchrotron radiation source. This method extends the lower limit of measurable viscosity using the falling sphere method at high pressure to 10^{-3} Pa s.

The highest viscosity that can be investigated by the falling sphere method may be expanded by the use of a centrifuge apparatus (Dorfman et al., 1996; Dorfman et al., 1997; Bagdassarov and Dorfman, 1998; Schmidt et al., 2006; Ardia et al., 2008). With viscosity and acceleration scaling linearly, a centrifugal force of 1000g expands the viscosity range to 10^{7} Pa s. The elevated acceleration (up to 1000g) also allows investigating viscosities between the solidus and the glass transition temperature (T_g). This kind of measurements are commonly performed on pure liquids. We are aware of only one published paper (Vetere et al. 2010) which investigated multiphase rheology of andesitic lavas under pressure conditions. In a few cases these experiments were run at acceleration of 1000g by means of centrifuge falling-sphere methods (e.g. Ardia et al., 2008).

A1.4. Paterson type apparata

The gold standard for quantitative high pressure deformation studies is the gas apparatus developed by Paterson (1970) and Paterson and Olgaard (2000). The apparatus can either compress

or extend the sample. Some gas apparatus, for example, the Paterson gas apparatus (Paterson, 1970), can also deform the sample in torsion. Torsion allows much higher strains to be reached. Because the amount of strain in the sample varies radically from the centre to the edge in torsion experiments, torsion samples are constructed in the shape of a thin ring with jacket materials filling the centre. What gives the gas apparatus its edge is that the gas confining medium (usually Ar) provides a perfect uniaxial stress field. Because the gas supports no shear tractions along the sides of the sample or pistons, an external load cell can accurately measure the load supported by the sample. Unfortunately, the gas apparatus can only achieve a confining pressure of 500 MPa (5 kbar). This pressure is equivalent to the pressure at 15 km depth in the earth. The limited pressure range is a severe limitation for students of the deep earth. Online resources: an Introduction to High Pressure Rock Deformation Techniques can be found at:

https://serc.carleton.edu/NAGTWorkshops/mineralogy/mineral_physics/deformation_mechanisms.html.

A1.5. Direct viscosity measurements on active flows in the field

Few direct measurements of lava rheology under natural conditions have been reported (Pinkerton and Sparks, 1978; Shaw et al., 1968; Belousov and Belousova, 2018; Chevrel et al. 2018). Nonetheless, some of these methods are based on the assumption of a parabolic velocity profile (Jeffrey's eq) and have the limitations highlighted at paragraph 3.2.1. These measurements are crucial for benchmarking of experimental data, but insufficient to develop a systematic understanding of the evolution of lava-flow properties in response to varying external and internal parameters (composition, cooling-and shear-rate, oxygen fugacity etc.), as they represent snapshots of the system at one specific condition (Belousov and Belousova, 2018). Belousov and Belousova, (2018) and Chevrel et al (2018) present the most recent technological advances of this unique technique and new field measurement results. Such direct measurements in the field require inserting a custom-built penetrometer, constituted by a steel bar with a half-spehrical penetration

head (e.g. Belousov and Belousova, 2018), or a viscometer (Chevrel et al., 2018), into the molten lava while it is flowing. Such in-situ viscometry is challenging due to the difficulty of accessing an active lava flow, and the lack of appropriate instrumentation. Measurements under such conditions are therefore very restricted and have mostly been performed on slow advancing lava flows and far from the solidification point of the lava.

1) During penetration viscometry (similar to that used to perform micropenetration experiment in the lab), where a rod is pushed into the liquid lava, the force required to penetrate the lava is kept constant and penetration is monitored with time until penetration ceases. Viscosity of lava is then calculated based on Stoke's law for half a sphere (i.e. the half spherical penetrating tip of the penetrating rod). Belousov and Belousova (2018) employed the relationship proposed by Panov (1988), according to which:

$$\eta_S\ (Pa \cdot s) = \frac{F}{3\pi v \mathrm{R}} \qquad \text{(A1.7)}$$

where F is the force (N), v is the speed of penetration (m/s) and R is the radius of the penetration head (m).

2) The rotational viscometry method, requires a shear vane to be inserted into the molten lava and the shear stress values corresponding to various applied rotation rates is measured. Viscosity is estimated as the shear stress over the strain-rate ratio ($\eta = \frac{\tau}{\dot{\gamma}}$). The shear stress ($\tau$) is calculated by: $\tau = \frac{M}{2\pi h R_i^2}$ where M is the torque recorded by the torque sensor, h is the length of the vane and R_i is the equivalent radius of the rotating vane assuming a wide gap concentric cylinder geometry. The strain-rate ($\dot{\gamma}$) is calculated according to the following formula: $\dot{\gamma} = \frac{2\omega}{n\left[1-\left(\frac{Ri}{Ro}\right)^{\frac{2}{n}}\right]}$

where ω is the rotational velocity (rad/s) and R_i and R_o are the inner and the outer radius of the spindle. n is the flow index which is determined by performing measurements at various rotational speed. The advantage of this approach is that it allows for evaluation of the lavas effective viscosity

922 at a range of shear rates. Viscosity estimates obtained by employing this procedure are reported in
923 Chevrel et al. (2018).

Appendix A2. Empirical and theoretical based formulations to express the T- and P-dependence of the viscosity of silicate liquids.

Among the known theoretical relations for coefficient of viscous flow of liquids, the Eyring arrhenian equation (Glasstone et al., 1941) is the most popular:

$$\eta = \eta_0 \exp(\Delta G/RT) \qquad \text{(Eq. A2.1);}$$

where R is the gas constant, T the absolute temperature and ΔG is the free activation energy of yield of the flow, that is, a function of the internal energy, entropy, P, and V (i.e. the volume of particles). The pre-exponential factor η_0, is related to the jump frequency of an atom from one sie to another and represent the microscopic view of the "viscosity". It can be expressed as $\eta_0 = hN_A / V_m$) where h is the Planck's constant, ($6.63\ 10^{-34}$ J s) and N_A the Avogadro's number ($6.02\ 10^{27}$) and V_m is the molar volume of the investigated liquid at very high temperature. This equation can be rewritten in logarithmic scale as it follows:

$$\log \eta = A + B/T \qquad \text{(Eq. A2.2);}$$

where $A=2.303*\log\eta_0$ and $B=\Delta G/R$. This Arrhenian form for viscosity has been used by Shaw (1972) and Bottinga and Weill (1972) to describe the first description of the viscosity of natural silicate melts.

Expansion of the melt viscometry database over a wider range of melt compositions and temperatures (closer to the so-called calorimetric glass transition temperature, T_g^{cal}, Angell, 1991; Scherer, 1984; Giordano et al., 2008a) exposed the limitations of Arrhenian models and new empirical and theoretical-based models have been provided to describe the temperature dependence of the viscosity of silicate liquids. In particular, the T–dependence of viscosity is accounted for by the three parameters in each of the most commonly employed formulation: (i) Vogel–Fulcher–Tamman (VFT)(Vogel, 1921; Fulcher, 1925; Tamman and Hesse, 1926); (ii) Adam–Gibbs (AG) (Adam and Gibbs, 1965) and (iii) Avramov (AV) (Avramov, 1998). These formulations accommodating the non-Arrhenian T -dependence of silicate melts, can be written as following:

949 Vogel–Fulcher–Tammann (VFT) : $\log \eta = A_{VFT} + B_{VFT}/(T - C_{VFT})$; (Eq. A2.3);
950 Adam and Gibbs (AG): $\log \eta = A_{AG} + B_{AG}/[T\, S^{conf}(T,x)]$; (Eq. A2.4);
951 Avramov (AV): $\log \eta = A_{AV} + (B_{AV}/T)^{CAV}$; (Eq. A2.5);
952
953 where η is the viscosity in Pa s, T is the absolute temperature, and A, B, C, D and S^{conf} (T,
954 x)(the so-called configurational entropy; representing the number of configurations accessible to the
955 liquids at the glass transition (Tg), Richet, 1984) are adjustable parameters (e.g. Giordano and
956 Russell, 2007; Giordano et al., 2008a, b; Russell and Giordano, 2017). The literature shows that, in
957 these systems, viscosity converges to a common value of the pre-exponential factors (A) that can be
958 assumed, at fixed pressure, to be independent of composition (e.g. Russell et al., 2003; Russell and
959 Giordano, 2005;; Giordano and Russell, 2007; Giordano et al., 2008a). The other adjustable
960 parameters in each equation are expanded to capture the effect of composition (Hui and Zhang,
961 2007; Giordano et al., 2008a). Several other formulations exist that can be reconciled with the three
962 model equation above mentioned. For instance, the most recent formulation of Mauro et al. (2009),
963 which is based on the AG theory, assumes that S^{conf} (T) is closely connected with the topological
964 degrees of freedom of atoms which provide an increased number of adjustable parameters. The
965 most recent GRD and HZ models used to describe the viscosity of anhydrous and volatile bearing
966 melts where B, C and S^{conf} parameters accommodate the effect of composition.

967
968 Empirical formulations used to constrain the effect of pressure on the viscosity of liquids
969 and characteristic parameters of Equations (Eqs. A2.1-A2.5) are provided by various authors (e.g.
970 Liebske et al., 2003; Ardia et al., 2008; Hui et al., 2009). In particular, Liebske et al (2003) by
971 modelling the viscosity of andesitic magmas and Ardia et al. (2008) modelling the viscosity of more
972 silicic magmas (rhyolites), used VFT expression (Eq. A2.3) where B_{VFT} parameter was function of
973 H_2O and cubic and a linear function of P, respectively, and C_{VFT} parameter was only function of
974 H_2O content and independent of P. Fig. A2.1 reports, as an example, the variation of viscosity at

975 constant T (1250 °C) as a function of P for melts of the Ab - Di system as fitted by using a linear
976 dependence from P of the B_{VFT} parameter.

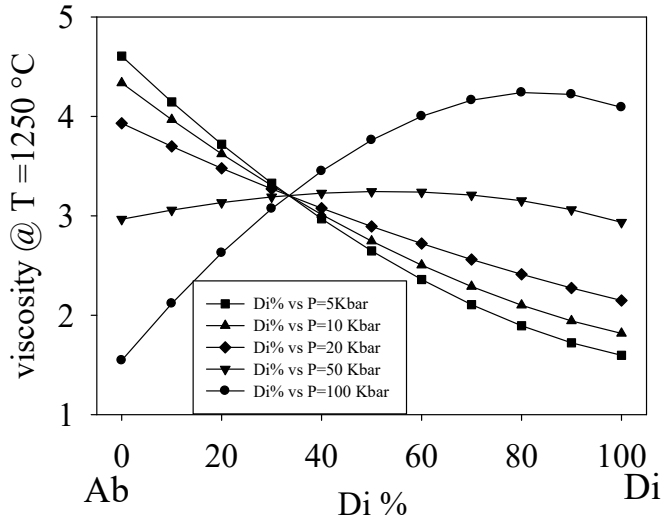

977
978 *Fig. A2.1. Isothermal viscosity variation as a function P (up to 100 kbar) for melts of the Ab-Di systems. The*
979 *viscosity was calculated here using VFT equation (Eq. A2.3) where the B_{VFT} = B0, VFT +b1*P(Kbar), where B0, VFT*
980 *is the pseudo-activation energy at 1 bar pressure and b1 is an adjustable parameter accounting for a linear P-*
981 *dependence of B_{VFT}. The effect of composition is shown in the figure. At T=1250 °C the pure liquid viscosity of the*
982 *albitic term (Ab100, left), proxy for a polymerized melt, is decreasing as P increases. On the other hand the pure liquid*
983 *viscosity for the diopsidic melt (Di100, right), proxy for more depolymerized compositions, increases as P increases.*
984

985 Online resources: a detailed summary of the philosophical approach employed to the construction
986 of the GRD model, predictable variables and downloadable versions of the viscosity calculator can
987 be found online at: https://www.eoas.ubc.ca/~krussell/VISCOSITY/grdViscosity.html

Appendix A3. Empirical formulations to express the effect of varying crystal/vesicle content, size and shape distributions and strain-rate on the viscosity of multiphase mixtures.

Viscosity is defined as the resistance to flow under specific applied stress (σ) conditions and it is expressed by complex functions of applied stress and resulting strain (γ) and strain-rates (e.g., Herschel and Bulkley, 1926). For a Newtonian liquid, $\sigma = \eta\dot{\gamma}$ where η is the Newtonian viscosity. It is well-kown from both laboratory studies on analogue materials (e.g. Mueller et al., 2011; Cimarelli et al, 2011; Truby et al., 2015) and natural remelted volcanic rock (e.g Caricchi et al., 2008; Vona et al., 2011; Campagnola et al., 2016; Kolzenburg et al., 2016; Soldati et al., 2016, 2017) that suspended solids and natural crystals lead to the increase of the suspension's bulk viscosity of up to several orders of magnitude compared to the solid particles free counterpart. On the other hand the role of an addition of bubbles on a suspension may lead to both a viscosity increase (spherical bubbles) or decrease (oblate deformed bubbles)(e.g. Llewellin et al., 2002). The presence of a solid phase or a gaseous phase to form a solid or bubble suspension commonly yield non-Newtonian behavior, expressed in the more general equation:

$$\sigma = \sigma_0 + K\dot{\gamma}^n \qquad \text{(Eq. A3.1)}$$

where σ_0 is a stress threshold (or yield stress) to be overcome in order to start flow; *K* is the flow consistency (which corresponds to shear viscosity at γ = 1 s^{-1}) and *n* is the flow index which describes the degree of non-Newtonian behavior, being equal to 1 for Newtonian fluids, *n*>1 for shear-thickening and *n*<1 for shear-thinning fluids. For non-Newtonian fluid (σ_0=0), the term $\sigma/\dot{\gamma}$ is equal to $K\dot{\gamma}^{n-1}$ and an apparent viscosity will be defined as $\eta_{app} = \sigma/\dot{\gamma}$, while the relative viscosity (η_r)(ratio between stress and strain rate divided by the viscosity of the suspending liquid, η_l) will be expressed by:

$$\eta_r = \left(\frac{K}{\eta_l}\right)\dot{\gamma}^{n-1} \qquad \text{(Eq. A3.2)}$$

where $K_r = K/\eta_l$ represents the relative consistency.

A3.1. Bubble-melt suspensions

When a bubble suspension flows bubble deformation is promoted, through the viscous forces, by shear (tending to deform bubbles) and opposed by surface tension which tends to restore/maintain bubble sphericity. The adimensional capillary number (*Ca*), i.e. the measure of the relative importance (i.e. the ratio) of shear and interfacial stresses, is: $Ca = \frac{\eta_{melt} \cdot r \cdot \dot{\gamma}}{\Gamma}$, where η_{melt}, r, $\dot{\gamma}$ and Γ are the viscosity of the suspension, the radius of the undeformed bubble, the shear rate of the flow and the liquid-vapour surface tension, respectively. The presence of bubbles can either increase or decrease the viscosity of a suspension depending on the dynamic regime (Manga et al., 1998; Lejeunne et al., 1999; Llewellin et al., 2002a,b; Rust and Manga, 2002; Stein and Spera, 2002; Llewellin and Manga, 2005). Similar to solid particles, bubbles deform flow lines within the suspending medium, which tends to increase the viscosity. However, at the same time, they provide free-slip surfaces which favour flow. For $Ca<1$, interfacial tension forces dominate and bubbles are approximately spherical (e.g., Taylor, 1932). In this case flow-line distortion is great and free-slip surface area is small, hence the overall effect is to increase the suspension viscosity. In contrast, at high deformation regimes, the bubbles will undergo significant elongation ($Ca>1$), thus favouring small flow-line distortion, greater free-slip surface area and a decrease in the suspension viscosity (Hinch and Acrivos, 1980, Llewellin and Manga, 2005; Vona et al., 2013, 2017).

However, the capillary number *Ca* implies an equilibrium between viscous and interfacial forces, and it can be applied only for steady flows, in which the conditions of shear have remained constant for a long enough time. As a consequence, if the shear strain rate is changing, the flow is unsteady and to describe unsteadiness Llewellin et al. (2002a, b) introduced the dynamic capillary number $Cd = \frac{\eta 0 \cdot r \cdot}{\tau} \frac{\ddot{\gamma}}{\dot{\gamma}}$, where the double derivative of strain-rate is the speed of strain-rate variation. For $Cd \ll 1$, the changes in shear environment are slow enough to allow the bubbles to reach their equilibrium shape, hence flow is steady and the dynamic regime is controlled by the capillary

number *Ca*. On the other hand, if *Cd*≫1, flow is unsteady, the bubbles are not able to reach their equilibrium shape in response to fast strain rate and they are, therefore, unrelaxed (they are actively deforming). In other words, in these conditions the rate of bubble deformation is large compared with the bulk strain rate and, therefore, most of the strain is accommodated by deformation of the gas in the bubbles. Since the gaseous phase has a negligible viscosity, this leads to a decrease of viscosity as the bubble content increases. Llewellin and Manga (2005) parameterized the effect of bubbles on the relative viscosity of a bubbly suspension, considering a single equation for the positive dependence of ηr on ϕb and a single equation for the negative dependence of ηr on ϕb, regardless of whether the decrease in viscosity in the latter case is related to steady (*Ca*>1) or unsteady (*Cd*>1) flow. Based on existing literature models (Bagdassarov and Dingwell, 1992, 1993; Pal 2003, Llewellin et al., 2002a,b), the authors suggested two different parameterizations for each viscous regime (increasing and decreasing η_r), considering two limiting cases corresponding to a minimum (MIN) and a maximum (MAX) effect of the bubbles on the viscosity of the suspensions.

For Ca<1 (increasing η_r):

$\eta_r=(1-\phi_b)^{-1}$ (MIN: Pal 2003); $\eta_r=(1+9\phi_b)$ (MAX: Llewellin, 2002a,b) (Eq. A3.13)

For Ca>1 or Cd>1 (decrasing η_r):

$\eta_r=(1-\phi_b)^{5/3}$(MIN: Pal 2003); $\eta_r=[1/(1+22.4\phi_b)]$ (MAX: Bagdassarov & Dingwell, 1992) (Eq. A3.14)

Online resources: a synthesis of the results obtained by Llewellin research can be found at the following webpage: http://community.dur.ac.uk/ed.llewellin/rheology.htm

Quane and Russell (2005), Russell and Quane (2005) and Robert et al (2008a, b) by performing uniaxial compression experiments on porous samples modelled the effective evolving viscosity (η_e) and porosity (φ) as from Russell and Quane (2005):

1061 $$\log \eta_e = \log \eta_0 - [\alpha\varphi/(1-\varphi)]^{\beta} \quad \text{(Eq. A3.15)}$$

1062 where α, β are unknown adjustable coefficients and η_o is the unknown effective viscosity of the
1063 melt plus crystal cargo at zero porosity. The parameter β was added to the original model of
1064 Ducamp and Raj (1989) to capture the full range of data and preserve a concave down equation
1065 form in the variables space (η, φ). The employed model was used to estimate the timescale for the
1066 welding of the block and ash flow deposits at Mount Meager. The results of the specific
1067 measurements of Quane and Russell (2005), Russell and Quane (2005), Robert et al (2008a, b) and
1068 new data on natural samples were compared by Vona et al. (2016) with the modelling proposed by
1069 Mader et al (2013), based on the analysis of analogue materials. Those results are in better
1070 agreement with the model proposed by Bagdassarov and Dingwell (1992). Finally, Vona et al.
1071 (2016) proposed a model to evaluate the strength of vesiculated magmas based on Eq. A3.15.

1072

1073 ***A3.2. Crystal-melt suspensions***

1074 In the last decades a significant number of experimental studies have investigated the
1075 rheological properties of different solid-bearing suspensions constituted by synthetic analogues
1076 (Mueller et al., 2011; Cimarelli et al., 2011; Moitra and Gonnermann, 2015; Truby et al., 2015;
1077 Klein et al., 2017, 2018; Dobson et al., 2015, 2016); synthetic silicate melts (Lejeune and Richet,
1078 1995; Caricchi et al., 2007; Champallier et al., 2008 and Costa et al., 2007a, 2009) and crystal-
1079 bearing natural magmas at subliquidus temperatures (e.g., Gay et al., 1969; Shaw, 1969; Marsh,
1080 1981; Ryerson et al., 1988; Pinkerton and Stevenson, 1992; Pinkerton and Norton, 1995; Sato,
1081 2005; Ishibashi and Sato, 2007; Caricchi et al., , 2008; Ishibashi, 2009; Vona et al., 2011, 2017;
1082 Campagnola et al., 2016; Kolzenburg et al., 2016, 2017, 2018).

1083 In crystal-melt suspensions, the dispersed phase acts as a 'hard' (non-deformable) inclusion
1084 which increases the viscosity of the suspension through both hydrodynamic and mechanical
1085 interaction among crystals. For low solid fractions, the viscosity increases slowly with the particle

volume fraction (ϕ), and the suspension maintains a Newtonian rheological behavior (strain-rate independent). When ϕ exceeds a critical value (ϕ_c), particles start to interact with each other and a solid network of particles begins to form, causing a strong increase in viscosity and the onset of non-Newtonian flow, characterized by Bingham-like rheology and/or shear thinning effects (Eq. (1)). As the solid fraction is further increased, the system reaches another rheological threshold, corresponding to the maximum packing density of solid particles (ϕ_m) Fig. 2), which causes the transition from melt and melt+crystal to solid-state creep rheology (e.g., Kohlstedt and Zimmerman, 1996; Lavallée et al., 2007, 2008, 2012). The value of ϕ_c is defined by both the crystal content as well as by the crystal size and crystal shape distributiosn (e.g. Costa et al., 2009; Cimarelli et al., 2011; Vona et al., 2011). The increase in viscosity and the non-Newtonian flow depend on textural features (crystal and bubble distribution) and deformation regimes (e.g., Costa et al., 2009; Petford, 2009; Mueller et al., 2011).

A number of models have been proposed describing the effect, on the suspensions rheology, of the crystal volume fraction and their,shape and size distributions as well as particles roughness and deformability (e.g., Einstein, 1906; Roscoe (1952); Maron and Pierce, 1956; Krieger and Dougherty, 1959; Frankel and Acrivos, 1970; Jeffrey and Acrivos, 1976; Marsh, 1981; McBirney and Murase, 1984; Costa, 2005; Hsueh and Becher, 2005; Stickel and Powell, 2005; Caricchi et al., 2007; Champallier et al., 2008; Costa et al., 2009; Ishibashi, 2009; Mueller et al., 2011; Cimarelli et al., 2011; Vona et al., 2011, Mader et al., 2013; Moitra and Gonnermann; 2015; Klein et al., 2017, 2018). The various models can be applied to represent the viscosity variation from a dilute ($\phi<0.03$, where viscosity increase is linear with crystal content and it is Newtonian) to a semi-dilute ($\phi<0.25$-$0.40<\phi_c$, where viscosity shows an increasing dependence of crystal fraction, but it is still Newtonian) until a concentrated regimes ($\phi_c<\phi<\phi_m$, for which viscosity shows a rapid increase and the onset of non-Newtonian rheology). For $\phi>\phi_m$ a solid creep-dominated rheology is observed until the occurrence of brittle failure. The crystal fraction ϕ at the transition between one and the

other regime depends strongly from the shape and size distributions (e.g. Saar et al., 2001; Costa et al., 2009).

So far, one of the most comprehensive models describing the relative viscosity variation from dilute to highly concentrated regimes is that proposed by Costa et al. (2009)(CM). According to that model:

$$\eta r(\phi) = \frac{1+\varphi^{\delta}}{[1-F(\varphi,\xi,\gamma)]^{B\phi^*}} \quad \text{(Eq. A3.3)}$$

where

$$F = (1-\xi)erf\left[\frac{\sqrt{\pi}}{2(1-\xi)}\varphi(1+\varphi^{\gamma})\right] \quad \text{(Eq. A3.4)}$$

with $\varphi = \phi/\phi^*$ where ϕ^*, ξ, γ and δ are adjustable parameters that depend on the deformation rate (Costa et al., 2009) and B is the Einstein coefficient (Einstein, 1906). The parameter ϕ^* represents the critical solid fraction at which the rheological transition from a dominant liquid phase regime switches to a regime where the effect of crystals is predominant and the viscosity values are much higher [Costa, 2005; Costa et al., 2009]. The CM is calibrated using suspensions containing crystal fractions, isotropically distributed, in the interval ϕ = 0.1 - 0.8.

Figure A2.1 shows, based on the Costa et al. (2009) model (CM), the strain-rate dependence of the relative viscosity at varying crystal volume fractions. The relative viscosity of two-phase mixture increases following a sigmoid curve with exponential increase above a critical solid fraction (ϕ_c), corresponding to the first inflection point in Fig. 2. This documents how variations of crystal content may cause orders of magnitude changes in suspension viscosity. A further important point in models of suspension rheology is that the maximum critical crystal volume fraction (ϕ_m) depends strongly on crystal shape, size distribution, crystal surface roughness and crystal orientation (e.g. Mueller et al., 2011; Mader et al., 2013; Klein et al., 2017; 2018). In general, ϕ_c and ϕ_m decrease with increasing crystal alignment and particle shape anisotropy (i.e., equant vs

elongated) and increases with dispersion in object size and surface roughness (e.g. Chong, 1971; Lejeune and Richet, 1995; Saar et al., 2001; Caricchi et al., 2007., 2008; Costa et al., 2009; Vona et al., 2011; Mueller, 2011; Mader et al., 2013; Klein 2018).

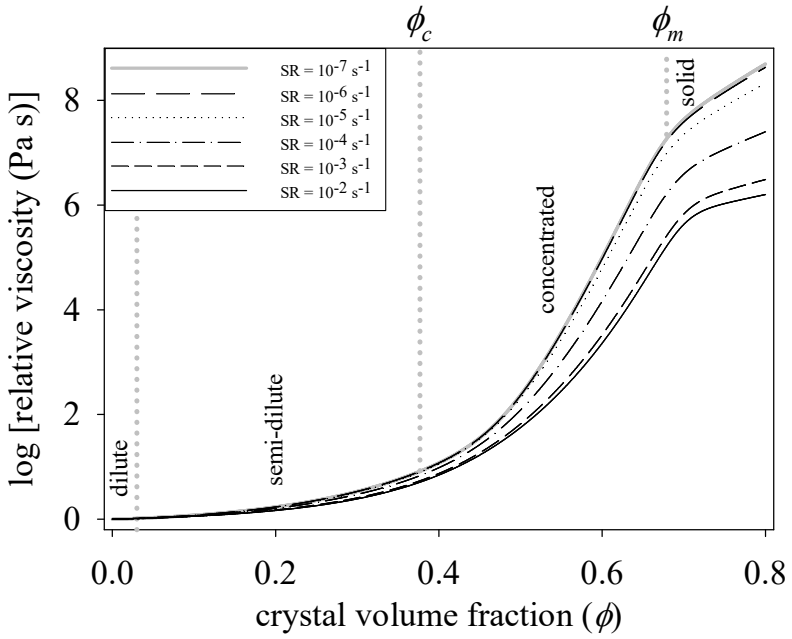

Fig. A.2.1. ***(a)*** *Relative viscosity as a function of crystal volume fraction of spheres at different strain-rates as calculated with the Costa et al. (2009) model. The figure shows, at first approximation, the inflection points at ϕ_c and ϕ_m, separating the semi-dilute, concentrated and solid-like deformation regimes and the dilute regime as described in the text. The inflection points are a function of the applied shear rates and shape and size distributions.*

Mueller et al. (2011) by studying the rheological response of monodisperse suspensions with different aspect ratios, and adopting the Maron-Pierce equation, where

$$\eta_r = \left(1 - \frac{\phi}{\phi_m}\right)^{-2} \qquad \text{(Eq. A3.5)}$$

concluded that both the flow index n and (Eq A3.1) the critical crystal fraction depend on the average particle aspect ratio (R), such that:

$$n = 1 - 0.2R\left(\frac{\phi}{\phi_m}\right)^4 \qquad \text{(Eq. A3.6)}$$

where the dependence of the ϕ_c from R-parameter is given, as in Mueller et al. (2011) by:

$$\phi_m = \frac{2}{0.321R+3.02} \quad \text{(Eq. A3.7)}$$

It is worth mentioning that the parameterization of Mueller et al (2011) and Mader et al. (2013) cannot extended above the critical solid fraction ϕ_m.Other authors (e.g Ishibashi, 2009; Mueller et al., 2011; Vona et al., 2011) proposed parameterizations obtained by modifications of the strain rate independent KD equation (Krieger and Dougherty, 1959)

$$\eta_r = \left(1 - \frac{\phi}{\phi_m}\right)^{-B\phi_m} \quad \text{(Eq. A3.8)}$$

to take into account the shear thinning effect on the rheology of suspensions. These authors provided modified strain rate dependent KD equations based on rheological measurements on low SiO_2 melts. Ishibashi (2009) provided the following expression for the relative viscosity:

$$\eta_r = \left(1 - \frac{\phi}{\phi_m}\right)^{-B_1\phi_m[1+\lambda\, ln(1-\phi/\phi_c)ln\dot{\gamma}]} \quad \text{(Eq. A3.9)}$$

where ϕ_m = 0.6 (as in the ER equation), B_1 = 5.46 represents the intrinsic (melt) viscosity at $\dot{\gamma}$ =1 s^{-1} and λ = 0.118 is an empirical constant which takes the shear thinning effect into account. In the Ishibashi (2009) parameterization, the fitting parameters were not related to the textural features of the suspensions (e.g., crystal shape, crystal shape dispersion, crystal size dispersion and orientation dispersion), such that the parameterization cannot be applied to other suspensions.

Later, Cimarelli et al. (2011) by using a KD expression extended the application of the parameterization provided by Mueller et al (2011) to account for bimodal shape polydispersion of particles.

Finally Vona et al. (2011) on the basis of rheological measurements on crystallizing polydispersed crystal-rich basalts provided a similar KD-derived parameterization

$$\eta_r = \left(1 - \frac{\phi}{\phi_m}\right)^{-2[1-\alpha log(\dot{\gamma})]} \quad \text{(Eq. A3.10)}$$

in which α is an empirical parameter equal to 0.06 and the effect of crystal shape can be evaluated using the equation proposed by Mueller et al. (2011) (Eq. (9)) where, in order to account for the disperse particle size distribution of the natural samples investigated, the average particles ratio ($\overline{R}$) is calculated by averaging the contribution of each group of particles having a certain aspect ratio and is called as it follows:

$$\bar{R} = \frac{\sum \phi_i \bar{R}_i}{\phi} \qquad \text{(Eq. A3.11)}$$

where ϕi and $\overline{R}_i$ are the crystal fraction and the mean aspect ratio of phase *i*. The model by Vona et al. (2011) is able to describe the rheological behavior of suspensions as a function of strain rate and textural features (i.e., crystal fraction, aspect ratios and shape polydispersion) and can be therefore applied to the complexities of natural magmas. An additional step ahead is provided by the work of Klein et al (2017, 2018) which express the critical crystal aspect ratio (ϕ_c) as a function of a polydispersity parameter (χ)(γ in Klein et al., 2018):

$$\phi_c = 1 - (1 - \phi_{c,0})\, \chi^{\alpha} \qquad \text{(Eq. A3.12)}$$

where $\phi_{c,0}$ represents the ϕ_c for a unimodal distribution of particles and α is an adjustable parameter (α = 0.173). The polydispersity employed is the ratio of the specific surface of a polydispersed system and that of a monodisperse system (Torquato, 2013; Wadsworth et al., 2017). Klein and coauthors employing Maron-Pierce kind of equation (Eq. A3.5) to express the relative viscosity and the parameterization of Mueller et al (2011) to account for the crystal ratio obtain and interesting expression for the relative viscosity of a polydisperse suspention and provide as supplementary material online an user-friendly spreadsheet .to calculate such a value (https://doi.org/10.1016/j.jvolgeores.2018.04.018).

A3.3. Three phase mixtures

Only few studies have explored the rheology of crystal and bubble-bearing magmas (e.g. Cordonnier et al., 2009; Pistone et al. 2012, 2013; 2015, 2016; Campagnola et al., 2016; Plese et al., 2018). Lavallée et al. (2007), Avard and Whittington (2011) have investigated natural lavas from domes by uniaxial deformation experiments. The authors have observed pseudo-plastic behavior with a strong shear thinning component for all the investigated magmas and provided equations describing the apparent viscosity as a function of temperature and strain rate for the multiphase magmas. Pistone et al. (2012) showed that three crystal and vesicle contents domains where non-Newtonian rheological behaviour varying from shear thinning (e.g. viscosity decreases as strain-rate increases and the flow index $n < 1$, Eq. A3.1) to shear thickening (e.g. viscosity increases as strain-rate increases and the flow index $n > 1$, Eq. A3.1) through intermediate between shear thickening and shear thinning were observed. The authors concluded that shear thinning occurred in crystal-rich suspensions (55-65 vol%) and bubble content of 9-10 vol% as due to crystal size reduction and shear localization. Shear tickening was instead observed in dilute suspensions (24 vol% crystal content, 12 vol% bubbles) as due to bubbles coalescence and boudinage which favoured water loss from the melts and sample degassing. Intermediate behaviour was observed for samples with 44 vol% crystals and 12 vol% bubbles probably due to the different temperatures and the time of experiments which did not give always time to the bubbles and crystal to orient along the flow lines, passing from prolate to oblate. The authors also showed that, caused by crystals and bubbles interactions, the interactions between flow-lines and crystals plus bubbles cannot be compared to that occurring for crystals and bubbles in only two-phase suspensions. Results from Pistone et al (2012) were applied to understand the process of viscous death and rejuvenation of magmatic bodies stored at depth (e.g. Bachmann and Bergantz, 2006).

The individual effect of crystal and bubbles was theoretically parameterized by Phan-Thien and Pham (1997) and later applied by Harris and Allen (2008) for the study of basaltic magmas

from Mauna Loa and Mount Etna. Depending on the relative size of crystals ($\Phi_{xtl,\ tot}$) and vesicles (Φb), Phan-Thien and Pham (1997) present three equations:

1. For crystals smaller than vesicles:

$$\eta = \eta_l \left(1 - \frac{\phi_{xtl,tot}}{1-\phi_b}\right)^{-\frac{5}{2}} (1 - \phi_b)^{-1} \qquad \text{(Eq. A3.16)}$$

2. For crystals and vesicles of equal size:

$$\eta = \eta_l \left[1 - \phi_{xtl,tot} - \phi_b\right]^{\frac{\left(-5\Phi_{xtl,tot}+2\Phi_b\right)}{\left(2\left(\Phi_{xtl,tot}+\Phi_b\right)\right)}} \qquad \text{(Eq. A3.17)}$$

3. For crystals larger than vesicles:

$$\eta = \eta_l \left(1 - \frac{\phi_b}{1-\phi_{xtl,tot}}\right)^{-1} \left(1 - \phi_{xtl,tot}\right)^{-\frac{5}{2}} \qquad \text{(Eq. A3.18)}$$

This treatment does not take into account the effect of textural variability, being applicable to spherical particles only, and strain rate dependency on the rheology.

Appendix A4. Equations to estimate rheological properties or constrain characteristic flow laws parameters starting from field observation of the geometrical features of lava flows.

Where direct measurement of the viscosity of lava flows (see A1.5) is not accessible the most accurate method to estimate the viscosity of lava flows is the so-called flow rate method (e.g. Kolzenburg et al., 2017, 2018a; Belousov and Belousova, 2018). Measuring accurately the flow rate of active lava flows allows calculating the apparent viscosities of the lava flows using Jeffreys' equations:

$$\eta = \rho g h^2 * \frac{sin(\alpha)}{3v} \textit{ (Eq. A4.1); } \eta = \rho g h^2 * \frac{sin(\alpha)}{2v} \textit{ (A4.2)}$$

where η is the viscosity of lava (Pa s), ρ is the bulk density (kg/ m3), g is the gravitational acceleration (9.8 m/s2), *h* is the thickness of the lava flow (m), α is the surface slope (degrees), and v is the velocity of lava flow (m/s). Eq. A4.1 is commonly used for data observing the flow front velocity, and the Eq. A4.2 is used for velocity observations of the flow surface behind the flow front (e.g. Nichols 1939; Gauthier 1973; Panov et al. 1988; Belousov nd Belousova, 2018). Measurements using this procedure are reported in several studies (e.g. Nichols 1939; Minakami 1951; Macdonald 1963; Einarsson 1966; Walker 1967; Gautier 1973; Andreev 1978; Fink and Zimbelman 1986; Vande-Kirkov 1987; Moore 1987; Panov 1988; Soldati 2016). Limitations of Jeffrey's equations have been discussed at 3.1.2.

Lava flow morphologies are thought, under particular assumptions, to reflect the rheological characteristic of the lavas (e.g., Wilson and Head, 1983; Hiesing et al., 2007). Assuming that: i) the rheological properties can be estimated from remote sensing data; ii) the geometry of the flow depends on lava rheology and that lava behaves as a Bingham fluid (i.e. a fluid whose rheological law is expressed by $\tau = \tau 0 + \eta * \dot{\gamma}$; where τ is the shear stress and τo is yield strength, that is, the shear stress necessary to first determine the beginning of the flow); iii) no inflation of the lava has occurred; then the yield strength of the lava flow (Pa) and the lava flow viscosity can be related to

its geometry according to the equations proposed by Moore et al. (1978). These equations, commonly employed in planetary science, have been recently adopted in numerous scientific contributions which also provide exhaustive reviews of the present state of art for the application of this method (e.g. Hiesinger et al., 2007; Chevrel et al., 2015; Castruccio et al., 2010, 2014; Kolzenburg et al., 2018a amongst the others). These contributions together with the new advances, due to comprehend the effect of crystalline and bubbles phases on the rheology of multiphase lavas, pointed out that this method, given the strong constitutive assumptions (in particular, single value of viscosity and yield strength during lava field evolution and emplacement), are not accurate enough to be employed, for instance, for real-time monitoring of lava flows (Chevrel et al., 2015).

References

Adam G., Gibbs J.H. (1965). On temperature dependence of cooperative relaxation properties in glass-forming liquids. J. Chem. Phys. 43, 139–146.

Andreev, V.I., Gusev, N.A., Kovalev, G.N., Slezin, Y.B. (1978). Dynamics of lava flows of southern breakthrough of great Tolbachik fissure eruption, 1975–76. Bull Volcanol Stations 55:18–26 (in Russian).

Angel, S.M., Gomer, N.R., Sharma, S.K. & McKay, C. (2012). Remote Raman Spectroscopy for Planetary Exploration: A Review. Applied Spectroscopy 66.

Angell, C.A., Relaxations in Complex Systems, (1995). U.S. Department of Commerce National Technical Information Service, ed. K. L. Ngai and G. B. Wright, 1985. pp. 3–11.

Angell, C.A. (1991). Relaxation in liquids, polymers and plastic crystals – strong fragile patterns and problems. J. Non-Cryst. Solids 131, 13–31.

Ardia, P., Giordano, D., Schmidt, M.W. (2008). A model for the viscosity of rhyolite as a function of H_2O-content and pressure: a calibration based on centrifuge piston cylinder experiments. Geochim. Cosmochim. Acta 72, 6103–6123.

Arzilli, F., Carroll, M.R. (2013). Crystallization kinetics of alkali feldspars in cooling and decompression-induced crystallization experiments in trachytic melt. Contrib. Miner. Petrol. 166, 1011-1027.

Audetat, A., Keppler, H. (2004). Viscosity of Fluids in Subduction Zones. Science 303, 513 – 516.

Avard, G., and Whittington, A. G. (2011). Rheology of arc dacite lavas: experimental determination at low strain rates. Bull. Volcanol. 74, 1039–1056.

Avramov I. (1998). Viscosity of glassforming melts. J. Non-Cryst. Solids 238, 6-10.

Bachmann, O. and Bergantz, G. (2006) Gas percolation in upper-crustal silicic crystaal crystal mushes as a mechanism for upward heat advection and rejuvination of near-solidus magma bodies. J. Volcanol. Geoth. Res. 149, 85 – 102.

Bagdassarov, N.S., Dingwell, D.B. (1992). A rheological investigation of vesicular rhyolite. J. Volcanol. Geoth. Res. 50, 307-322.

Bagdassarov, N.S., Dingwell, D.B. (1993). Deformation of foamed rhyolites under internal and external stresses: an experimental investigation. Bull. Volcanol. 55, 147-154.

Bagdassarov, N., and H. Pinkerton (2004). Transient phenomena in vesicular lava flows based on laboratory experiments with analogue materials. J. Volcanol. Geoth. Res. 132, 115 – 136.

Bagdassarov, N. and Dorfman, A. (1998). Granite rheology: magma flow and melt migration. J. Geol. Soc. 155, 863-872.

Baker, D.R., Vaillancourt, J. (1995). The Low Viscosities of F+ H_2O-Bearing Granitic Melts and Implications for Melt Extraction and Transport. Earth Planet. Sci. Lett. 132, 199-211.

Behrens, H. and Schulze, F. (2003). Pressure dependance of melt viscosity in the system $NaAlSi_3O_8$-$CaMgSi_2O_6$. Am. Min. 88, 1351-1363.

Belousov, A., and M. Belousova. (2018). Dynamics and Viscosity of ’A ’ā and Pāhoehoe Lava Flows of the 2012-2013 Eruption of Tolbachik Volcano, Kamchatka (Russia). Bull. Volcanol. 80.

Belousov A, Belousova M, Edwards B, Volynets A, Melnikov D (2015). Overview of the precursors and dynamics of the 2012–13 basaltic fissure eruption of Tolbachik Volcano, Kamchatka, Russia. J. Volcanol. Geotherm. Res. 307, 22–37.

Bernstein, M., Pavez, A., Varley, N,, Whelley, P., Calder, E. (2013). Rhyolite lava dome growth styles at Chaitén volcano, Chile (2008-2009): interpretation of thermal imagery. Andean Geol 40, 295–309.

Bertin, D., Lara, L.E, Basualto, D., Amigo, Á., Cardona, C., Franco, L., Gil, F., Lazo, J. (2015) High effusion rates of the Cordón Caulle 2011–2012 eruption (southern Andes) and their relation with the quasi-harmonic tremor. Geophys. Res. Lett. 42, 7054–7063.

Bottinga, Y., Weill, D. (1972). The viscosity of magmatic silicate liquids: a model for calculation. Am. J. Sci. 272, 438–475.

Brearley, M., Dickinson, J. E., Scarfe, C. M. (1986). Pressure-Dependence of Melt Viscosities on the Join Diopside-Albite. Geochim. Cosmochim. Acta 50, 2563-2570.
Brearley, M. and Montana, A. (1989). The Effect of Co2 on the Viscosity of Silicate Liquids at High-Pressure. Geochim. Cosmochim. Acta 53, 2609-2616.
Burnham, C.W. (1963). Viscosity of a water rich pegmatite. Spec. Pap. Geol. Soc. Am. 76, 26.
Campagnola, S., Vona, A., Romano, C., Giordano, G. (2016). Crystallization kinetics and rheology of leucite-bearing tephriphonolite magmas from the Colli Albani volcano (Italy). Chem. Geol. 424, 12-29.
Canon-Tapia, E., Walker G. (2004). Global aspects of volcanism: the perspectives of ''plate tectonics'' and ''volcanic systems''. Earth Sci. Rev. 66, 163–182.
Cañón-Tapia, E. (2016). Reappraisal of the significance of volcanic fields. J. Volcanol. Geotherm. Res. 310, 26-38.
Caricchi, L., Burlini, L., Ulmer, P., Gerya, T., Vassalli, M., Papale, P. (2007). Non-Newtonian rheology of crystal-bearing magmas and implications for magma ascent dynamics. Earth Planet. Sci. Lett. 264, 402–419.
Caricchi, L., Giordano, D., Burlini, L., Ulmer, P., Romano, C. (2008). Rheological properties of magma from the 1538 eruption of Monte Nuovo (Phlegrean Fields, Italy): an experimental study. Chem. Geol. 256, 158–171.
Carn SA, Pallister JS, Lara L, Ewert JW, Watt S, Prata AJ, Thomas RJ, Villarosa G (2009). The unexpected awakening of Chaitén volcano, Chile. EOS Trans Am Geophys Union 90, 205–206
Cashman, K.V., Thornber, C., Kauahikaua, J.P. (1999). Cooling and crystallization of lava in open channels, and the transition of P¯ahoehoe Lava to'A'¯a. Bull. Volcanol. 61, 306–323.
Cashman KV, Soule S, Mackey B, Deligne N, Deardorff N, Dietterich H (2013). How lava flows: New insights from applications of lidar technologies to lava flow studies. Geosphere 9, 1664-1680.
Castro, J. Schipper, C.I. Mueller, S.P. Militzer, A.S., Amigo, A. et al. (2013). Storage and eruption of near-liquidus rhyolite magma at Cordón Caulle, Chile. Bull. Volcanol. 75, 1-17.
Castruccio, A., Rust, A.C., Sparks R.S.J. (2010). Rheology and flow of crystal-bearing lavas: Insights from analogue gravity currents. Earth Planet. Sci. Lett. 297, 471–480.
Castruccio, A, Rust, AC Sparks, RSJ (2014). Assessing lava flow evolution from post-eruption field data using Herschel-Bulkley rheology. J. Volcanol. Geoth. Res. 275, 71-84.
Champallier, R., Bystricky, M., Arbaret, L. (2008). Experimental investigation of magma rheology at 300 MPa: From pure hydrous melt to 75 vol. % of crystals, Earth Planet. Sci. Lett. 267, 571–583.
Chang, C., Powell, R.L. (1994). Effect of particle size distributions on the rheology of concentrated bimodal suspensions. J. Rheol. 38, 85–98.
Chevrel, M.O., Platz, T., Hauber, E., Baratoux, D., Lavallée, Y., Dingwell, D.B. (2013a). Lava flow rheology: a comparison of morphological and petrological methods. Earth Planet. Sci. Lett. 384, 109–120.
Chevrel, M.O., Giordano, D., Potuzak, M., Courtial, P., Dingwell, D.B. (2013b). Physical properties of CaAl2Si2O8–CaMgSi2O6–FeO–Fe2O3melts: analogues for extra-terrestrial basalt. Chem. Geol.346, 93–105.
Chevrel, M.O., Cimarelli, C., deBiasi, L., Hanson, J.B., Lavallée, Y., Arzilli, F., Dingwell, D.B., (2015). Viscosity measurements of crystallizing andesite from Tungurahua volcano (Ecuador). Geochem. Geophys. Geosyst. 16, 870–889.
Chevrel, M.O., Harris, A., James, M., Gurioli, L., Patrick, M. (2017). Measuring the viscosity of lava using a field rheometer. MemoVolc Meeting Abstract. 21 – 23 February, 2017, Catania, Italy.
Chevrel, M.O., Harris, A.J.L., James, M.R., Calabrò, L., Gurioli, L., Pinkerton, H. (2018). The viscosity of pāhoehoe lava: In situ syn-eruptive measurements from Kilauea, Hawaii. Earth and Planetary Science Letters, 493, 161-171.
Chong, J.S., Christiansen E.B., Baer, A.D. (1971). Rheology of concentrated suspensions. J. Appl. Polym. Sci.15, 2007–2021.

Cimarelli, C., Costa, A., Mueller, S., Mader, H.M. (2011). Rheology of magmas with bimodal crystal size and shape distributions: Insights from analog experiments. Geochemistry Geophysics Geosystems 12, 1-14.
Coats, R., Cai, B., Kendrick, J., Wallace, P., Hornby, A., Miwa, T., von Aulock, F., Ashworth, J., Godinho, J., Atwood, R. (2017). Understanding the rheology of two and three-phase magmas. In: AGU Fall Meeting Abstracts.
Coish, R., and Taylor, L.A. (1979) The effects of cooling rate on texture and pyroxene chemistry in DSDP Leg 34 basalt: a microprobe study. Earth and planetary science letters, 42(3), 389-398.
Coppola, D., Piscopo, M.L.D., Cigolini, C. (2013). Rheological Control on the Radiant Density of Active Lava Flows and Domes. 239, 39 – 48.
Coppola, D., Laiolo, M., Franchi, A., Massimetti, F., Cigolini, C., Lara, L.E. (2017). Measuring effusion rates of obsidian lava flows by means of satellite thermal data. J. Volcanol. Geoth. Res. 347, 82 – 90.
Cordonnier, B., Hess, K.-U., Lavallée, Y., and Dingwell, D.B. 2009. Rheological properties of dome lavas: Case study of Unzen volcano. Earth and Planetary Science Letters 279, 263–272.
Cordonnier, B., Schmalholz, S. M., Hess, K.-U., Dingwell, D. B. (2012). Viscous heating in silicate melts: An experimental and numerical comparison. J. Geophys. Res. 117, B02203.
Costa, A., Macedonio, G. (2003). Viscous heating in fluids with temperature-dependent viscosity: implications for magma flows. Nonlinear Processes in Geophysics 10, 545-555.
Costa, A. (2005). Viscosity of high crystal content melts: dependence on solid fraction. Geophysical Research Letters 32, 5.
Costa A., Macedonio G. (2005). Computational modeling of lava flows: A review. Geological Society of America Special Papers 396, 209-218.
Costa, A., Macedonio, G. (2005). Numerical simulation of lava flows based on depth-averaged equations. Geophysical Res. Lett. 32, L05304.
Costa, A, Melnik O.,Vedeneeva E. (2007a). Thermal effects during magma ascent in conduits. J. Gepophys. Res. 112, B12205.
Costa, A, Melnik O., R.S.J. Sparks (2007b). Controls of conduit geometry and wallrock elasticity on lava dome eruptions. Earth Planet. Sci. Lett 260, 137 – 151;
Costa, A., Caricchi, L., Bagdassarov, N.S., (2009). A model for the rheology of particle bearing suspensions and partially molten rocks. Geochem. Geophys. Geosyst. 10, 1–13.
Del Gaudio, P., Behrens, H., Deubener, J. (2007). Viscosity and glass transition temperature of hydrous float glass. Journal of Non-Crystalline Solids 353, 223-236.
Del Negro, C., Fortuna, L., Herault, A., Vicari, A. (2008). Simulations of the 2004 lava flow at Etna volcano by the MAGFLOW Cellular Automata model. Bull Volc. 70, 805 - 812.
Del Negro, C., Cappello, A., Neri, M., Bilotta, G., Herault, A., Gnci, G. (2013). Lava flow hazards at Mount Etna: constraints imposed by eruptive history and numerical simulations. Sci. Rep. 13, 3493.
Del Negro, C., Cappello, A., Ganci, G. (2016). Quantifying lava flow hazards in response to effusive eruption. GSA Bull. 128, 752-763.
Di Genova, D., Kolzenburg, S., Wiesmaier, S., Dallanave, E., Neuville, D., Hess, K-U, Dingwell, D.B. (2017). A chemical tipping point governing mobilization and eruption style of rhyolitic magma. Nature 552, 235 – 238.
Dingwell DB (1986). Viscosity-temperature relationships in the system Na2Si2O5-Na4Al2O5. Geochim. Cosmochim. Acta 50,1261-1265.
Dingwell DB (1989). Shear viscosities of ferrosilicate liquids. American Mineralogist (9-10):1038-1044.
Dingwell, D.B., Virgo, D., (1987). The effect of oxidation state on the viscosity of melts in the system Na_2O-FeO-Fe_2O_3-SiO_2. Geochimica et Cosmochimica Acta 51, 195-205.

Dingwell, D.B., Virgo, D., (1988). Viscosities of melts in the Na_2O-FeO-Fe_2O_3-SiO_2 system and factors controlling relative viscosities of fully polymerized silicate melts. Geochim. Cosmochim. Acta 52, 395-403.
Dingwell, D.B., Bagdassarov, N.S., Bussod, G.Y, Webb, S.L. (1993). Magma Rheology. Am. Min. Ass. Can., Short Course Handbook 21, 131 – 196.
Dingwell, D.B. (1996). Volcanic dilemma: flow or blow? Science, 273, 1054-1055;
Dobson K, Pistone M, Fife J, Cordonnier B, Blundy J, Dingwell D, Lee P (2015). Quantifying dynamic rheology, phase interactions and strain localisation in deforming three phase magmas using high-speed x-ray tomography. In: EGU General Assembly Conference Abstracts.
Dobson K, Wadsworth F, Di Genova D, Kolzenburg S, Vasseur J, Marone F, Dingwell D (2016). Magmas on the Move: in situ 4D Experimental Investigation into the Rheology and Mobility of Three-Phase Magmas Using Ultra Fast X-ray Tomography. In: AGU Fall Meeting Abstracts.
Dorfman, A., Hess, K.-U., Dingwell, D. B. (1996). Centrifuge-assisted falling-sphere viscometry. Eur. J. Mineral. 8, 507-514.
Dorfman, A., Dingwell, D. B., Bagdassarov, N. S. (1997). A rotating autoclave for centrifuge studies: falling sphere viscometry. Eur. J. Mineral. 9, 345-350.
Dragoni, M. (1993). Modelling the rheology and cooling of lava flows, in Active Lavas: Monitoring and Modelling, edited by C. R. J. Kilburn and G. Luongo, pp. 235– 261, Univ. Coll. of London Press, London.
Dragoni, M., Borsari, I., Tallarico, A. (2005). A model for the shape of lava flow fronts. J. Geophys. Res., 110, B09203, doi:10.1029/2004JB003523.
Einstein, A. (1906). A new determination of molecular dimensions. Ann. Phys. 19, 289 – 306.
Einarsson T (1966) Studies of temperature, viscosity, density and some types of materials produced in the Surtsey eruption. Surtsey Res Progr Rep 1, 163–179.
Farquharson, J., James, M., Tuffen, H. (2015). Examining rhyolite lava flow dynamics through photo-based 3D reconstructions of the 2011–2012 lava flowfield at Cordón-Caulle, Chile. J. Volcanol. Geotherm. Res. 304, 336–348.
Faxèn, H. (1922). The resistance against the movement of a rigour sphere in viscous fluids, which is embedded between two parallel layered barriers. Annalen Der Physik 68, 89-119.
Filippucci, M., Tallarico, A., Dragoni, M. (2013). Role of heat advection in a channeled lava flow with power law, temperature-dependent rheology. J. Geophys. Res. 118, 2764 – 2776.
Filippucci, M., Tallarico, A., Dragoni, M. (2018). Far-field boundary conditions in channeled lava flow with viscous dissipation. An. Geophys. 61, ag-7782, this issue
Fink, J. H., J. R. Zimbelman (1986). Rheology of the 1983 Royal Gardens basalt flows, Kilauea volcano, Hawaii. Bulletin of Volcanology 48, 87-96.
Flynn, L.P., and Mouginis-Mark, P.J. (1992). Cooling rate of an active Hawaiian lava flow from nighttime spectroradiometer measurements. Geophysical Research Letters, 19(17), 1783-1786.
Frankel, N.A., Acrivos A. (1970). A versatile parallel-plate viscometr for glass viscosity measurement to 1000°C. J. Fluid Mech. 44, 65 – 78.
Fulcher GS 1925 J. Am. Ceramic Soc. 8 339-355.
Gamble, R.P., and Taylor, L.A. (1980). Crystal/liquid partitioning in augite: effects of cooling rate. Earth Planet. Sci. Lett. 47, 21-33.
Gay, E.C., Nelson, P.A., Armstrong, W.P. (1969). Flow properties of suspensions with high solids concentration. Aiche Journal 15, 815-822.
Gauthier, F. 1973. "Field and Laboratory Studies of the Rheology of Mount Etna Lava. Philosophical Transactions of the Royal Society of London A: Mathematical, Physical and Engineering Sciences 274, 83–98.
Gent, A.N. (1960). Theory of parallel plate viscometer. Brit. J. Appl. Phys. 11, 85 – 88.
Giordano, D. and Dingwell, D. B. (2003a). Non-Arrhenian multicomponent melt viscosity: a model. Earth Planet. Sci. Lett. 208, 337-349.

Giordano, D., Dingwell, D.B. (2003b). The kinetic fragility of natural silicate melts. J. Phys.: Condens. Matter 15, S945–S954.
Giordano, D., Nichols, A.R.L., Dingwell, D.B. (2005) Glass transition temperatures of natural hydrous melts: a relationship with shear viscosity and implications for the welding process. J. Volcanol. Geoth. Res. 142, 105–118.
Giordano, D., Polacci, M., Longo, A., Papale, P., Dingwell, D., Boschi, E., Kasereka, M. (2007). Thermo-rheological magma control on the impact of highly fluid lava flows at Mt. Nyiragongo. Geophys. Res. Lett. 34. L06301.
Giordano, D., Mangicapra, A., Potuzak, M., Russell, J.K., Romano, C., Dingwell, D.B., Di Muro, A. (2006). An expanded non-Arrhenian model for silicate melt viscosity: A treatment for metaluminous, peraluminous and peralkaline melts. Chem. Geol. 229, 42–56.
Giordano, D., Russell, J.K., (2007). A rheological model for glassforming silicate melts in the systems CAS, MAS, MCAS. J. Phys. Condens. Matter 19, 205148.
Giordano, D., Russell, J.K., Dingwell, D.B. (2008a). Viscosity of magmatic liquids: a model. Earth Planet. Sci. Lett.271, 123–134.
Giordano, Potuzak M, Romano C, Dingwell DB, Nowak M (2008b). Viscosity and glass transition temperature of hydrous melts in the system $CaAl_2Si_2O_8$–$CaMgSi_2O_6$. Chemical Geology 256, 203-215.
Giordano, D., Ardia, P., Romano, C., Dingwell, D.B., Di Muro, A., Schmidt, M.W., Mangiacapra, A., Hess K-U. (2009). The rheological evolution of alkaline Vesuvius magmas and comparison with alkaline series from the Phlegrean Fields, Etna, Stromboli and Teide. Geochim. Cosmochim. Acta 73, 6613– 6630.
Giordano D., La Felice S., Arzilli F., De Cristofaro S.P., Masotta M., Polo L. (2017). Il vulcanismo effusivo acido del Monte Amiata: stima delle condizioni pre-eruttive ed implicazioni vulcanologiche. Effusive acidic volcanism of Monte Amiata: estimates of pre- and syn-eruptive conditions and volcanological implications. Capitolo monografia Amiata. ISBN 978-88-99742-32-4.
Giordano, D., Russell, J.K. (2018). Toward a Structural Model for the Viscosity of Geological Melts. Earth Planet. Sci. Lett. 501, 202-212.
Giordano, D., González-García, D., Russell, J.K, Raneri, S., Bersani, D., Fornasini, L., Di Genova, D., Ferrando, S., Kaliwoda, M, Lottici, P.P., Smit ., and Dingwell, D.B. (2019). A calibrated database of Raman spectra for natural silicate glasses: implications for modelling melt physical properties. Accepted
Glasstone, S., Laidler, K.J., Eyring, H. (1941). The Theory of Rate Processes. McGraw-Hill, New-York.
Hammer, J.E. (2006). Influence of fO_2 and cooling rate on the kinetics and energetics of Fe-rich basalt crystallization. Earth and Planetary Science Letters, 248(3), 618-637.
Harris, A.J., Allen, J.S. III (2008). One-, two- and three-phase viscosity treatments for basaltic lava flows. J Geophys Res. 1;113. pii: B09212.
Herschel, W.H., Bulkle, R. (1926). Konsistenzmessungen von Gummi-Benzollösungen. Kolloid Z. 39:291–300.
Hess, K.-U., and Dingwell, D.B. (1996). Viscosities of hydrous leucogranitic melts: A non-Arrhenian model. Am. Min. 81, 1297-1300.
Hess, K.-U., Cordonnier, B., Lavallée, Y., and Dingwell, D.B. (2008) Viscous heating in rhyolite: An in situ experimental determination. Earth Planet. Sci. Lett. 275, 121-126.
Hiesinger, H., Head III, J.W., Neukum, G. (2007). Young lava flows on the eastern flank of Ascreus Mons: Rheological properties derived from High Resolution Stereo Capera (HRSC) images and Mars Orbiter Laser Altimeter (MOLA) data. J. Geophy. Res. 112, E05011, doi:10.1029/2006JE002717;
Hinch, E. J. & Acrivos, A. 1980 Long slender drops in a simple shear flow. J. Fluid Mech. 98, 305.

Hon, K, J Kauahikaua, R Denlinger, and K Mackay. 1994. “Emplacement and Inflation of Pahoehoe Sheet Flows: Observations and Measurements of Active Lava Flows on Kilauea Volcano, Hawaii.” Geol. Soc. Am. Bull. 106: 351–70.
Hui, H.J., Zhang, Y. (2007). Toward a general viscosity equation for natural anhydrous and hydrous silicate melts. Geochim. Cosmochim. Acta 71, 403-416.
Hui, H., Zhang, Y., Xu, Z., Del Gaudio, P., Behrens, H. (2009). Pressure dependence of viscosity of rhyolitic melts. Geochim. Cosmochim. Acta 73, 3680 – 3693.
Hulme, G. (1974). The interpretation of lava flow morphology, Geophys. J. R. Astron. Soc., 39, 361– 383.
Hsueh. C.H., Becher, P.F. (2005). Effective Viscosity of Suspensions of Spheres. J. Am. Ceram. Soc. 88, 1046 – 1049.
Ishibashi, H. and Sato, H. (2007). Viscosity measurements of subliquidus magmas: Alkali olivine basalt from the Higashi-Matsuura district, Southwest Japan. J. Volcanol. Geoth. Res. 160, 223 - 238
Ishibashi, H. (2009). “Non-Newtonian Behavior of Plagioclase- Bearing Basaltic Magma: Subliquidus Viscosity Measurement of the 1707 Basalt of Fuji Volcano, Japan.” J. Volcanol. Geoth. Res. 181: 78–88.
James, M. R., Pinkerton, H., Robson., R. (2007). Image-Based Measurement of Flux Variation in Distal Regions of Active Lava Flows.” Geochemistry, Geophysics, Geosystems 8 (3). doi:10.1029/2006GC001448.
Jeffrey, H. (1925). The flow of water in an inclined channel of rectangular section. Philos. Mag. J. Sci. 49, 793 – 807.
Jeffrey, D.J., Acrivos, A. (1976). The rheological properties of suspensions of rigid particles. - AIChE Journal, 1976 - Wiley Online Library
Kanzaki, M., Kurita, K., Fujii, T., Kato, T., Shimomura, O., Akimoto, S. (1987). A new technique to measure the viscosity and density of silicate melts at high pressure. In: Manghnani, M. H. a. S., S. (Ed.), High-Pressure research in Mineral Physics, Washington.
Kahle, A., Winkler, B., Hennion, B. (2003). Is Faxe´n’s correction function applicable to viscosity measurements of silicate melts with the falling sphere method?. J. Non-Newtonian Fluid Mech. 112 203–215.
Kilburn, C.R.J. (2015). Chapter 55 - Lava Flow Hazards and Modeling A2 - Sigurdsson, Haraldur. In: The Encyclopedia of Volcanoes (Second Edition). Academic Press, Amsterdam, pp 957-969.
Klein, J., Mueller, S.P., Castro, J.M. (2017). The influence of crystal size distribution on the rheology of magmas: new insights from analogues experiments. Geochem. Geophys. Geosyst, 18.
Klein, J., Mueller, S.P., Helo, C., Schweitzer, S., Gurioli, L., Castro, J.M. (2018). An expanded model and application of the combined effect of crystal-size distribution and crystal shape on the relative viscosity of magmas. J. Volcanol. Geoth. Res. 357, 127 – 133.
Kohlstedt, D.L., & Zimmerman, M. E. (1996). Rheology of partially molten mantle rocks. Annual Review of Earth and Planetary Sciences, 24, 41-62.
Kolzenburg, S., Favalli, M., Fornaciai, A., Isola, I., Harris, A.J.L., Nannipieri, L., Giordano, D. (2016a). Rapid Updating and Improvement of Airborne LIDAR DEMs Through Ground-Based SfM 3-D Modeling of Volcanic Features. IEEE Transactions on Geoscience and Remote Sensing 99, 1-13.
Kolzenburg, S., Giordano, D., Cimarelli, C., Dingwell, D.B. (2016b) In Situ thermal characterization of cooling/crystallizing lavas during rheology measurements and implications for lava flow emplacement. Geochim. Cosmochim. Acta 195, 244-258.
Kolzenburg, S., Giordano, D., Thordarson, T., Höskuldsson, A., Dingwell, D.B. (2017). The rheological evolution of the 2014/2015 eruption at Holuhraun, central Iceland. Bull. Volcanol. 79, 45.
Kolzenburg, S., Jaenicke, J., Münzer, U., Dingwell, D.B. (2018a). The effect of inflation on the morphology-derived rheological parameters of lava flows and its implications for interpreting

remote sensing data - A case study on the 2014/2015 eruption at Holuhraun, Iceland. J. Volc. Geoth. Res. 357, 200-212.
Kolzenburg S., Di Genova D., Giordano D., Hess K.U., Dingwell D.B. (2018b). The effect of oxygen fugacity on the rheological evolution of crystallizing basaltic melts. Earth Planet. Sci. Lett. 487, 21 – 32.
Kolzenburg, S.; Giordano, D., Di Muro, A., Dingwell, D.B. (2019). Equilibrium Viscosity and Disequilibrium Rheology of a high Magnesium Basalt from the 2007 eruption of Piton De La Fournaise volcano, La Reunion, Indian Ocean, France. AG, this issue.
Kolzenburg, S.; Giordano, D., Hess, K.U., Dingwell, D.B. (2018d). Shear Rate-Dependent Disequilibrium Rheology and Dynamics of Basalt Solidification. 10.1029/2018GL077799
Kouchi, A., Tsuchiyama, A., Sunagawa, I. (1986). Effect of stirring on crystalization kinetics of basalt: Texture and element partitioning. Contrib. Mineral. Petrol. 93, 429 – 438.
Krieger, I. and Dougherty, T. (1959). A mechanism for non-Newtonian flow in suspension of rigid sphere. Trans. Soc. Rheol., 3, 137 – 152.
Kushiro, I. (1976). Changes in Viscosity and Structure of Melt of $NaAlSi_2O_8$ Composition at High Pressures. Journal of Geophysical Research 81, 6347-6350.
Kushiro, I., Yoder, J., H.S., Mysen, B. O. (1976). Viscosities of Basalt and Andesite Melts at High Pressures. Journal of Geophysical Research 81, 6351-6356.
Kushiro, I. (1977). Phase Transformation in silicate melts under upper-mantle conditions. In: Akimoto, M. H. M. a. S. (Ed.), High Pressure Research Applications in Geophysics.
Kushiro, I. (1978). Viscosity and structural changes af Albite (NaAlSi3O8) melt at high pressures. Earth Planet. Sci. Lett. 41, 87-90.
Lara L.E. (2009). The 2008 eruption of the Chaitén volcano, Chile—a preliminary report. Andean Geol 36, 125–129
La Spina, G., Burton, M., Vitturi, M.D.M. (2015). Temperature evolution during magma ascent in basaltic effusive eruptions: a numerical application to Stromboli volcano. Earth Planet. Sci. Lett.426, 89–100.
La Spina, G., Burton, M., Vitturi, M.D.M., Arzilli, F. (2016). Role of syn-eruptive plagioclase disequilibrium crystallization in basaltic magma ascent dynamics. Nature Communications 7, 13402.
Lavallée, Y., Hess, K.-U., Cordonnier, B., Dingwell, D.B. (2007). Non-Newtonian rheological law for highly crystalline dome lavas. Geology 35, 843.
Lavalleé, Y., Meredith, P.G., Dingwell, D.B., Hess, K. U., Wassermann, J., Cordonnier, B., Gerik, A. and Kruhl, J.H. (2008). Seismogenic lavas and explosive eruption forecasting. Nature 453, 507–510.
Lejeune, A.M., and P. Richet (1995). Rheology of crystal-bearing silicate melts: An experimental study at high viscosities, J. Geophys. Res., 100, 4215–4229.
Lejeune, A.M., Bottinga, Y., Trull, T.W., Richet, P. (1999). Rheology of bubble-bearing magmas, Earth Planet. Sci. Lett. 166, 71–84.
LeLosq, C., Neuville, D. (2017). Molecular structure, configurational entropy and viscosity of silicate melts: Link through the Adam and Gibbs theory of viscous flow. J. Non-Cryst. Solids 463, 175-188.
Liebske, C., Behrens, H., Holtz, F. Lange, R. (2003). The influence of pressure and composition on the viscosity of andesitic melts. Geochim. Cosmochim. Acta 67, 473 – 485.
Liebske, C, Schmickler, B., Terasaki, H., Poe, B., Suzuki, A., Funakoshi, K.I, Ando, R., Rubie, D.C. (2005). Viscosity of peridotite liquid up to 13 GPa: Implications for magma ocean viscosities. Earth Planet. Sci. Lett. 240, 589 – 604.
Llewellin, E.W., Mader, H.M., Wilson, S.D.R., (2002a). The rheology of a bubbly liquid. Proc. R. Soc. London, Ser. A 458, 987–1016.
Llewellin, E.W., Mader, H.M., Wilson, S.D.R. (2002b). The constitutive equation and flow dynamics of bubbly magmas. Geophys. Res. Lett. 29:23.1–23.4, (doi:10.1029/2002GL015697).

Llewellin, E.W., Manga, M., 2005. Bubble suspension rheology and implications for conduit flow. J. Volcanol. Geotherm. Res. 143, 205–217.
Lofgren, G. (1980.) Experimental studies on the dynamic crystallization of silicate melts. Physics of magmatic processes, 487.
Long, P.E., and Wood, B.J. (1986). Structures, textures, and cooling histories of Columbia River basalt flows. Geological Society of America Bulletin, 97, 1144-1155.
Mader, H.M., Llewellin, E.W., Mueller, S.P. (2013). The rheology of two-phase magmas: A review and analysis. J. Volcanol. Geoth. Res. 257, 135-15
Manga, M., J. Castro, K. Cashman, and M. Loewenberg (1998). Rheology of bubble-bearing magmas, J. Volcanol. Geoth. Res., 87, 15–28.
Magnall N, James MR, Tuffen H, Vye-Brown C (2016) Similarities in basalt and rhyolite lava flow emplacement processes. Geophys Res Abstr 18:9199
Magnall N, James MR, Tuffen H, Vye-Brown C (2017) Emplacing a cooling limited rhyolite flow. Volcanic and Magmatic Studies Group Annual Meeting, Liverpool, Abstr, p 141
Maron, S.H. and Pierce, P.E. (1956). Application of ree-eyring generalized flow theory to suspensions of spherical particles. J. Colloid Sci. 11, 80–95.
Marsh B.D. (1981). On the crystallinity, probability of occurrence, and rheology of lava and magma. Contrib. Mineral. Petrol. 78, 85–98.
Mauro, J.C. , Yue, Y. , Ellison,, A.J. , Gupta P.K. , Allan D.C. (2009). Proc. Natl. Acad. Sci. USA., 106, 19780
McBirney, A.R., Murase, T. (1984). Rheological properties of magmas. Ann. Rev. Sci. 12, 337 – 357.;
Melnik, O., and Sparks, R.S.J. (1999). Nonlinear dynamics of lava dome extrusion. Nature 402, 37 – 41.
Melnik, O. and Sparks, R.S.J. (2005). Controls of conduit magma flow dynamics during lava dome building eruptions. J. Geophys. Res. 110, B02209.
Melnik, O., Sparks, R.S.J., Costa, A., Barmin, A.A. (2009). Volcanic Eruptions: Cyclicity during Lava Dome Growth. Encyclopedia of Complexity and Systems Science 9763 -9784.
Minakami, T., Ishikawa, T., Yagi, K. (1951). The 1944 eruption of Volcano Usu in Hokkaido, Japan. Bull. Volcanol. 11, 45 – 157.
Moitra, P. and Gonnermann, H.M. (2015). Effects of crystal shape- and size-modality on magma rheology. Geochemistry, Geophysics, Geosystems, 16, 1-26.
Moore, H., Arthur, D., Schaber, G. (1978). Yield Strengths of Flows on the Earth, Mars, and Moon, Lunar and Planetary Science Conference Proceedings. pp. 3351–3378.
Morgavi, D., Petrelli, M., Vetere, F., González-García, D., Perugini, D. (2015). High-temperature apparatus for chaotic mixing of natural silicate melts. Review of Scientific Instruments 86(10):105108.
Mueller, S., Llewellin, E.W., Mader, H.M. (2011). The rheology of suspensions of solid particles. Proc. R. Soc. London, Ser. A 466, 1201–1228.
Naboko, S.I. (1947). Bilyukai Eruption in 1938. Tr Lab Vulkanol 5:122– 134.
Németh, K. (2010). Monogenetic volcanic fields: origin, sedimentary record, and relationship with polygenetic volcanism. Geological Society of America Special Papers, 470, 43-66.
Nicolas, A. and Ildefonse, B. (1996). Flow mechanism and viscosity in basaltic magma chambers. Geophys. Res. Lett. 23, 2013-2016.
Nichols, R L. (1939). Viscosity of Lava. The Journal of Geology 47, 290–302.
Ohtani, E., Suzuki, A., Ando, R., Urakawa, S., Funakoshi, K., Katayama, Y. (2005). Viscosity and density measurements of melts and glasses at high pressure and temperature by using the multi-anvil apparatus and synchrotron X-ray radiation. In: Advances in High-Pressure Technology for Geophysical Applications. Elsevier, pp 195-209
Pal, R. (2003). Rheological behavior of bubble-bearing magmas. Earth Planet. Sci. Lett. 207, 165-179. doi: 10.1016/S0012-821X(02)01104-4.

Pallister, J.S., Diefenbach, A.K., Burton, W.C., Muñoz, J., Griswold, J.P., Lara, L.E., Lowenstern, J.B., Valenzuela, C.E. (2013). The Chaitén rhyolite lava dome: eruption sequence, lava dome volumes, rapid effusion rates and source of the rhyolite magma. Andean Geol 40(2):277–294
Panov VK, Slezin YB, Storcheus AV (1988) Mechanical properties of lava extruded in the 1983 Predskazanny eruption (Klyuchevskoi volcano). J Volcanol Seismol 7:25–37
Papale, P., (1999). Strain-induced magma fragmentation in explosive eruptions. Nature (London) 397, 425–428.
Paterson, M.S., (1970). Experimental Rock Deformation—The Brittle Field, 13. Springer-Verlag, Berlin–Heidelberg–New York.
Paterson, M.S. (1978). Experimental Rock Deformation—The Brittle Field, 13. Springer-Verlag, Berlin–Heidelberg–New York.
Paterson, M.S., Olgaard, D.L. (2000). Rock deformation tests to large shear strains in torsion. Journal of Structural Geology 22, 1341–1358.
Pedersen, G.B.M., et al. (2017). Lava field evolution and emplacement dynamics of the 2014–2015 basaltic fissure eruption at Holuhraun, Iceland. J. Volcanol. Geotherm. Res 340, 155–169.
Persikov, E.S., Zharikov, V.A., Bukhitiyarov, P.G., Polskoy, S.F. (1990). The effect of volatiles on the properties of mgmatic melts. Eur. J. Mineral. 2, 621 – 642.
Petford, N. (2009) Which effective viscosity? Mineral. Magazine 73, 167 - 171
Phan-Thien, N., and Pham, D.C. (19979. Differential multiphase models for polydispersed suspensions and particulate solids. Journal of Non-Newtonian Fluid Mechanics, 72, 305–318.
Piermarini GJ, Forman RA, Block S. (1978). Viscosity measurements in the diamond anvil pressure cell. Rev. Sci. Instrum. 49, 1061
Pinkerton, H, and R S J Sparks. (1978). “Field Measurements of the Rheology of Lava.” Nature 276: 383–85.
Pinkerton, H, and R J Stevenson. (1992). “Methods of Determining the Rheological Properties of Magmas at Sub-Liquidus Temperatures.” Journal of Volcanology and Geothermal Research 53: 47–66.
Pinkerton, H, Wilson, L. (1994). Factors controlling the lengths of channel-fed lava flows. Bull.Volcanol. 56, 108 – 120.
Pinkerton, H, Norton, GE (1995). 'Rheological properties of basaltic lavas at sub-liquidus temperatures: laboratory and field-measurements on lavas from Mount Etna. J. Volcanol. Geoth. Res. 68, 307-323
Pistone, M., Caricchi, L., Ulmer, P., Burlini, L., Ardia, P., Reusser, E., Marone, F., Arbaret, L. (2012). Deformation experiments of bubble- and crystal-bearing magmas: rheological and microstructural analysis. J. Geophys. Res. 117. http://dx.doi.org/10. 1029/2011JB008986.
Pistone, M., Caricchi, L., Ulmer, P., Burlini, L., Reusser, E., and Ardia, P. (2013). Rheology of volatile-bearing crystal mushes: mobilization vs. viscous death. Chem. Geol., 345, 16–39.
Pistone M, Arzilli F, Dobson KJ, Cordonnier B, Reusser E, Ulmer P, Marone F, Whittington AG, Mancini L, Fife JL (2015). Gas-driven filter pressing in magmas: Insights into in-situ melt segregation from crystal mushes. Geology 43(8):699-702
Pistone, M., Cordonnier, B., Ulmer, P., Caricchi, L. (2016). Rheological flow laws for multiphase magmas: an empirical approach. J. Volcanol. Geotherm. Res. 321, 158–170.
Pleše P, Higgins M, Mancini L, Lanzafame G, Brun F, Fife J, Casselman J, Baker D (2018). Dynamic observations of vesiculation reveal the role of silicate crystals in bubble nucleation and growth in andesitic magmas. Lithos 296:532-546
Pocklington, H.C. (1940). Rough measurement of high viscosities. Proceedings of the Cambridge Philosophical Society 36, 507-508.
Polacci M., Papale P., Del Seppia D., Giordano D. and Romano C. (2004) Dynamics of magma ascent and fragmentation in trachytic versus rhyolitic eruptions. J. Volcanol. Geoth. Res. 131, 93–108.

Polacci, M, Arzilli, F, La Spina, G, Le Gall, N, Caiet, B, Hartley, M.E., Di Genova, D., Vo, N.T., Nonni, S., Atwood, R.C., Llewellin, E.W., Lee, P.D. and Burton, M.R. (2018). Crystallisation in basaltic magmas revealed via in situ 4D synchrotron X-ray microtomography. Nature

Polacci M, Mancini L, Baker DR (2010). The contribution of synchrotron X-ray computed microtomography to understanding volcanic processes. Journal of synchrotron radiation 17, 215-221.

Polo L.A., Giordano D., Janasi V., Freitas-Guiaraes L. (2018). Effusive silicic volcanism in in the Paraná Magmatic Province, South Brazil: Physico-chemical conditions of storage and eruption and considerations on the rheological behaviour during emplacement. J. Volcanol. Geoth. Res. 355, 115 - 135.

Polo L.A., Janasi V., Giordano D., E. Canon Tapia, E. Lima, M. Roverato. (2018). Effusive silicic volcanism in the Paraná Magmatic Province, South Brazil: evidence for local fed lava flows and domes from detailed field work. J. Volcanol. Geoth. Res. 355, 204 – 218.

Quane SL, Russell JK (2005) Welding: insights from high-temperature analogue experiments. J Volcanol Geotherm Res 142, 67–87.

Ratteron P, Merkel S (2009). In situ rheological measurements at extreme pressure and temperature using synchrotron X-ray diffraction and radiography. Journal of synchrotron radiation 16, 748-756.

Rhéty M, Harris A, Villeneuve N, Gurioli L, Médard E, Chevrel O, Bachélery P (2017). A comparison of cooling-and volume-limited flow systems: Examples from channels in the Piton de la Fournaise April 2007 lava flow field. Geochemistry, Geophysics, Geosystems

Richet, P. (1984). Viscosity and configurational entropy of silicate melts. Geochim. Cosmochim. Acta 48, 471–483.

Richet, P., Bottinga, Y. (1995). In Structure, Dynamics and Properties of Silicate Melts, eds. J.F. Stebbins, P.F. McMillan and Dingwell DB, Rev. Mineral. 32, 67-94.

Richet, P., Lejeune, A.-M., Holtz, F., Roux, J. (1996). Water and the viscosity of andesite melts. Chem. Geol. 128, 185-197.

Robert; G., Russell, J.K., Giordano, D. (2008a). Rheology of porous volcanic materials: High-temperature experimentation under controlled water pressure. Chem. Geol., 256, 215-229.

Robert; G., Russell, J.K., Giordano, D., Romano, C. (2008b). High-T deformation of volcanic materials in the presence of water. American Mineralogist 93, 74-80.

Robert B, Harris A, Gurioli L, Médard E, Sehlke A, Whittington A (2014) .Textural and rheological evolution of basalt flowing down a lava channel. Bulletin of Volcanology 76, 1-21.

Roscoe, R. (1952). The viscosity of suspensions of rigid spheres. British Journal of Applied Physics 3, 306

Russell, J.K., Giordano, D., Dingwell, D.B., Hess, K.U., 2002. Modelling the non-Arrhenian rheology of silicate melts: Numerical considerations. Eur. J. Mineral. 14, 417–427.

Russell, J. K., Giordano, D., Dingwell, D. B. (2003). High-temperature limits on viscosity of non-Arrhenian silicate melts. Am. Min. 88, 1390-1394.

Russell, J.K., Giordano, D. (2005). A model for silicate melt viscosity in the System CaMgSi2O6–$CaAl_2Si_2O_8$–$NaAlSi_3O_8$. Geochim. Cosmochim. Acta 69, 5333–5349.

Russell J.K. and Quane S.L. (2005). Rheology of welding: inversion of field constraints. J. Volcanol. Geoth. Res. 142,173 – 191.

Russell, J.K., Giordano, D. (2017). Modelling configurational entropy of silicate melts. Chemical Geology 461, 140-151.

Ryan and Blevins, 1987

Ryerson, F.J., Weed, H.C., Piwinskii, A.J. (1988). Rheology of subliquidus magmas: 1. Picritic compositions. J. Geophys. Res.: Solid Earth, 93 (B4), 3421-3436

Ryan, A., Kolzenburg, S., Vona, A., Heap, M., Russell, JJ.K. (2019). A proxy for magmatic foams: FOAMGLAS®, a closed-cell glass insulation. J. non-Cryst. Solids: X, 1

Rust, A.C., Manga, M. (2002). Bubble Shapes and Orientations in Low Re Simple Shear Flow. J. Coll. Inter. Sci. 249, 476 – 480.

Saar, M. O., M. Manga, K. V. Cashman, and S. Fremouw (2001). Numerical models of the onset of yield strength in crystal-melt suspensions, Earth Planet. Sci. Lett., 187, 367–379.
Sato, H. (2005), Viscosity measurement of subliquidus magmas: 1707 basalt of Fuji Volcano, J. Mineral. Petrol. Sci., 100, 133–142.
Scarfe, C.M., Mysen, B.O., Virgo, D. (1987). Pressure dependence of the viscosity of silicate melts. In: Magmatic processes: Physicochemical Principles. Geochem. Soc. Spec. Pub. 1, 59 -67.
Scherer, G.W. (1984). Use of the Adam-Gibbs equation in the analysis of structural relaxation, J. Am. Ceram. Soc. 67, 504 - 511.
Schipper CI, Castro JM, Tuffen H, James MR, How P (2013) Shallow vent architecture during hybrid explosive–effusive activity at Cordón Caulle (Chile, 2011–12): evidence from direct observations and pyroclast textures. J Volcanol Geotherm Res 262:25–37
Schmidt M. W., Connolly J. A. D., Gu¨nther D. and Bogaerts M. (2006) Element partitioning: the role of melt structure and composition. Science 312, 1646–1650.
Sehlke A, Whittington A, Robert B, Harris A, Gurioli L, Médard E (2014) Pahoehoe to `a`a transition of Hawaiian lavas: an experimental study. Bulletin of Volcanology 76(11):1-20
Shaw, H R, T L Wright, D L Peck, and R Okamura. 1968. "The Viscosity of Basaltic Magma: An Analysis of Field Measurements in Makaopuhi Lava Lake, Hawaii." American Journal of Science 266: 225–64.
Shaw, H R. (1969). "Rheology of Basalt in the Melting Range." J. Petrol. 10, 510–535.
Shaw H. R. (1972) Viscosities of magmatic silicate liquids: An empirical model of prediction. Am. J. Sci. 272, 438–475.
Soldati A, Sehlke A, Chigna G, Whittington A (2016). Field and experimental constraints on the rheology of arc basaltic lavas: the January 2014 Eruption of Pacaya (Guatemala). Bulletin of Volcanology 78(6):1-19
Soldati, A., Beem J., Gomez F., Huntley J.W., Robertson T., Whittington A. (2017). Emplacement dynamics and timescale of a Holocene flow from the Cima Volcanic Field (CA): Insights from rheology and morphology. J. Volc. Geoth. Res. 347, 91 -111.
Song S-R, Jones KW, Lindquist BW, Dowd BA, Sahagian DL (2001). Synchrotron X-ray computed microtomography: studies on vesiculated basaltic rocks. Bulletin of Volcanology 63(4):252-263
Sparks, R.S.J. (2004). Dynamics of magma degassing. Volcanic degassing. Geol. Soc. Lond.Spec. Pub. 213, 5–22.
Stein, D.J., Spera, F.J (2002). Shear viscosity of rhyolite-vapor emulsions at magmatic temperatures by concentric cylinder rheometry J. Volcanol. Geoth. Res. 113, 243 – 258.
Suzuki A., Ohtani E., Terasaki H. and Funakoshi K. (2005). Viscosity of silicate melts in CaMgSi2O6–NaAlSi2O6 system at high pressure. Phys. Chem. Minerals 32, 140–145.
Tammann, G. and Hesse, W. (1926). Die Abhängigkeit der Viskosität von der Temperatur bei unterkühlten Flüssigkeiten. Zeitschrift für anorganische und allgemeine Chemie 156, 245-257;
Taniguchi H. (1995). Universal viscosity-equation for silicate melts over wide temperature and pressure ranges. J. Vol. Geoth. Res. 66, 1–8.
Tobolsky, A.V. and Taylor, R.B. (1963). Viscoelastic properties of a simple organic glass. J. Phys. Chemistry 67, 2439-2442.
Torquato, S., (2013). Random Heterogeneous Materials: Microstructure and Macroscopic Properties. Vol. 16. Springer Science & Business Media.
Truby, J.M., Mueller, S.P., Llewellin, E.W., Mader, H.M. (2015). The rheology of three-phase suspensions at low bubble capillary number. Proc. R. Soc. A 471 (2173):20140557. https://doi.org/10.1098/rspa.2014.0557.
Tuffen H, James M.R., Castro J.M. Schipper C.I. (2013). Exceptional mobility of an advancing rhyolitic obsidian flow at Cordo´n Caulle volcano in Chile. Nature Communication. DOI: 10.1038/ ncomms3709

Vande-Kirkov YV (1978). Viscosity of the lavas of the Northern Breakthrough (Tolbachik), 1975. Bull Volcanol Stations 55, 13–17.
Vetere F., Behrens H., Holtz F. and Neuville D. R. (2006). Viscosity of andesitic melts-new experimental data and a revised calculation model. Chem. Geol. 228, 233–245.
Vetere F., Behrens H., Holtz F., Vilardo G., Ventura G. (2010). Viscosity of crystal-bearing hydrous andesites and its implication for magma ascent. Journal of Mineralogical and Petrological Sciences 105, 151-163.
Vetere, F., Sato H., Ishibashi H., De Rosa R., Donato P. (2013). Viscosity Changes during Crystallization of a Shoshonitic Magma: New Insights on Lava Flow Emplacement. J. Mineralogical and Petrological Sciences 108, 144–160.
Vetere, F., Rossi, S., Namur, O., Morgavi, D., Misiti, V., Mancinelli, P., Petrelli, M., Pauselli, C., Perugini, D. (2017). Experimental constraints on the rheology, eruption and emplacement dynamics of analog lavas comparable to Mercury's northern volcanic plains. Journal of Geophysical Research: Planets
Vogel, D.H. (1921). Temperaturabhängigkeitsgesetz der Viskosität von Flüssigkeiten. Physikalische Zeitschrift 22, 645-646.
Vona, A., Romano, C., Dingwell, D.B., Giordano, D. (2011). The rheology of crystal-bearing basaltic magmas from Stromboli and Etna. Geochim. Cosmochim. Acta 75, 3214–3236.
Vona, A., Romano, C., Giordano, D., Russell, J.K. (2013a). The multiphase rheology of magmas from Monte Nuovo (Campi Flegrei, Italy). Chem. Geol. 346, 213 – 227.
Vona A., Romano C. (2013). The effects of undercooling and deformation rates on the crystallization kinetics of Stromboli and Etna basalts. Contrib. Mineral. Petrol. 166, 491-509.
Vona, A., Ryan, A., Russell, J.K., Romano, C. (2016). Models for viscosity and shear localization in bubble-rich magmas. Earth Planet. Sci. Lett. 449, 26 -38.
Vona, A., Di Piazza, A., Nicotra, E., Romano, C., Viccaro, M., Giordano G. (2017). The complex rheology of megacryst-rich magmas: The case of the mugearitic “cicirara” lavas of Mt. Etna volcano. Chem. Geol. 458, 48-67.
Wadsworth, F.B., Vasseur, J., Llewellin, E.W., Dingwell, D.B. (2017). Sintering of polydisperse viscous droplets. Phys. Rev. E 95, 033114-1, 033114-7.
Walker, D., Kirkpatrick, R., Longhi, J., Hays, J. (1976). Crystallization history of lunar picritic basalt sample 12002: phase-equilibria and cooling-rate studies. Geol. Soc. Am. Bull. 87, 646-656
Wieczorek, M.A., Zuber, M.T, Phillips, R.J. (2001). The role of magma buoyancy on the eruption of lunar basalts. Earth Planet. Sci. Lett. 185, 71-83
Whittington, A., Richet, P., Holtz, F. (2000). Water and the viscosity of depolymerized aluminosilicate melts. Geochim. Cosmochim. Acta 64, 3725-3736.
Whittington, A., Richet, P., Linard, Y., Holtz, F., (2001) The viscosity of hydrous phonolites and trachytes. Chem. Geol. 174, 209-223.
Whittington, A., Bouhifd, M.A., Richet, P. (2009). The viscosity of hydrous NaAlSi3O8 and granitic melts: Configurational entropy. Am. Min. 94, 1–16.
Wilson, L., Head J.W (2016). Generation, ascent and eruption of magma on the Moon: New insights into source depths, magma supply, intrusions and effusive/explosive eruptions (Part 1: Theory). Icarus 283, 146-175.
Witter, J.B., Harris A.J. (2007). Field measurements of heat loss from skylights and lava tube systems. J. Geophys. Res.: Solid Earth 112, 1978–2012.